Geochemistry Geophysics Geosystems G3
AN ELECTRONIC JOURNAL OF THE EARTH SCIENCES
Published by AGU and the Geochemical Society

Article
Volume 4, Number 4
23 April 2003
9003, doi:10.1029/2002GC000412
ISSN: 1525-2027

Record of forearc devolatilization in low-T, high-P/T metasedimentary suites: Significance for models of convergent margin chemical cycling

Seth J. Sadofsky

Department of Earth and Environmental Sciences, 31 Williams Drive, Bethlehem, Lehigh University, Pennsylvania 18015, USA

Currently at Forchungszentrum GEOMAR, Wischhofstr 1-3, 24148 Kiel, Germany. (ssadofsky@geomar.de)

Gray E. Bebout

Department of Earth and Environmental Sciences, 31 Williams Drive, Lehigh University, Bethlehem, Pennsylvania 18015, USA

[1] The Franciscan Complex (Coast Ranges and Diablo Range, California) and the Western Baja Terrane (WBT; Baja California, Mexico) were metamorphosed along high-P/T paths like those experienced in many active subduction zones, recording peak conditions up to ~1 GPa and 300°C. Franciscan and WBT metasedimentary rocks are similar in lithology and geochemistry to clastic sediments outboard of many subduction zones. These metamorphic suites provide evidence regarding devolatilization history experienced by subducting sediments, information that is needed to mass-balance the inputs of materials into subduction zones with their respective outputs. Analyzed samples have lower total volatile contents than their likely protoliths. Little variation in LOI among similar lithologies at differing metamorphic grades, suggests that loss of structurally bound water occurred during early clay-mineral transformations. Finely disseminated carbonate is present in the lowest-grade rocks, but absent in all higher-grade rocks. $\delta^{13}C_{VPDB}$ of reduced-C is uniform in the lower-grade Franciscan samples (mean = −25.1‰, 1σ = 0.4‰), but varies in higher-grade rocks (−28.8 to −21.9‰). This likely reflects a combination of devolatilization and C-isotope exchange, between organic and carbonate reservoirs. Nitrogen concentration ranges from 102 to 891 ppm, with $\delta^{15}N_{air}$ of +0.1 to +3.0‰ (n = 35); this organic-like $\delta^{15}N$ probably represents an efficient transfer of N from decaying organic matter to reacting clay minerals. The lowest-grade rocks in the Coastal Belt have elevated carbonate contents and correlated N-$\delta^{15}N$ variations, and exhibit the most uniform $\delta^{13}C$ and C/N, all consistent with these rocks having experienced less devolatilization. Most fluid-mobile trace elements are present at concentrations indistinguishable from protoliths. Suggesting that, despite apparent loss of much clay-bound H_2O and CO_2 from diagenetic cements (combined, <5–10 wt. %), most fluid-mobile trace elements are retained to depths of up to ~40 km. Organic-like $\delta^{15}N$, lower than that of many seafloor sediments, is consistent with some loss of adsorbed N (perhaps as NO_3^-) during early stages of diagenesis. The efficient entrainment of fluid-mobile elements to depths of at least 40 km in these relatively cool subduction zone settings lends credence to models invoking transfer of these elements to the subarc mantle.

Components: 16,645 words, 17 figures, 5 tables.

Keywords: Subduction-zone; metamorphism; nitrogen-isotope; carbon-isotope; devolatilization; trace elements.

Index Terms: 1030 Geochemistry: Geochemical cycles (0330); 1040 Geochemistry: Isotopic composition/chemistry; 3660 Mineralogy and Petrology: Metamorphic petrology.

Received 23 July 2002; **Revised** 16 January 2003; **Accepted** 31 January 2003; **Published** 23 April 2003.

Sadofsky, S. J., and G. E. Bebout, Record of forearc devolatilization in low-T, high-P/T metasedimentary suites: Significance for models of convergent margin chemical cycling, *Geochem. Geophys. Geosyst.*, *4*(4), 9003, doi:10.1029/2002GC000412, 2003.

Theme: Trench to Subarc: Diagenetic and Metamorphic Mass Flux in Subduction
Guest Editors: Gray Bebout and Tim Elliott

1. Introduction

[2] Subduction zones provide the mechanism for the transport of sedimentary rocks and altered seafloor basalt to the mantle, and are the only geochemical pathway for material to return to the mantle from the crust, oceans, and atmosphere (Figure 1). Metamorphic devolatilization is regarded as one of the main factors that control the cycling of the volatile elements on Earth [e.g., *Berner et al.*, 1983; *Kerrick and Caldeira*, 1993], and the extent to which rocks are devolatilized during subduction remains a fundamental question in the understanding of geochemical cycles. Metamorphism of volatile-rich rocks in forearc to subarc regions of subduction zones probably dictates the extent to which elements are released to return to the surficial system or retained and recycled back into the mantle [*Bebout*, 1995, 1996].

[3] Investigation of subduction-zone metamorphic rocks [see *Bebout*, 1991; *Moran et al.*, 1992; *Moran*, 1993; *Bebout et al.*, 1993, 1999] has shown that the retention or loss of volatile and relatively fluid-mobile elements is strongly dependent on the prograde P-T paths that the rocks experience, and thus the thermal structure of the subduction zone. Study of the Catalina Schist has demonstrated that rocks metamorphosed along higher-T, prograde paths show dramatic devolatilization resulting in significant decrease in the concentrations of some relatively fluid-mobile trace elements (e.g., B, Cs, As, and Sb; see *Bebout et al.* [1999]). However, work on the lowest-grade (lawsonite-albite and lawsonite-blueschist facies) metasedimentary rocks in the Catalina Schist pointed to some subtle variation in extents of devolatilization related to differing prograde histories, and an overall high degree of retention of volatiles in rocks experiencing the low-T prograde paths [see *Bebout et al.*, 1999]. In this study we further test the hypothesis that the relatively cool subduction, characteristic of many modern Earth convergent margins, can promote efficient subduction of volatile components to depths approaching 50 km, the maximum depths recorded by the voluminous metasedimentary parts of circum-Pacific paleoaccretionary suites. Field localities in the Franciscan Complex and the Western Baja Terrane contain lithologies that are similar to those outboard of many active subduction zones and have experienced metamorphism at a range of high-P/T conditions thought to be representative of thermal regimes in modern convergent margins (see thermal models of *Peacock* [1992, 1996]). Here we compare the chemical compositions of low-T metasedimentary rocks of the Franciscan Complex and Western Baja Terrane with those of their likely protoliths, evaluate the extents of devolatilization experienced during the prograde metamorphism of these rocks, and briefly discuss the significance of the inferred devolatilization effects for the convergent margin cycling of volatiles and relatively fluid-mobile elements.

2. Geologic Settings and Mineralogy

[4] The Franciscan complex (Northern California, USA; see Figure 2) and Western Baja Terrane (exposed on Cedros Island, Baja California, Mexico) were selected as field localities for this study because they contain abundant, well-preserved, metasedimentary rocks that have experienced prograde P-T conditions like those expected for relatively cool subduction zones. In the California

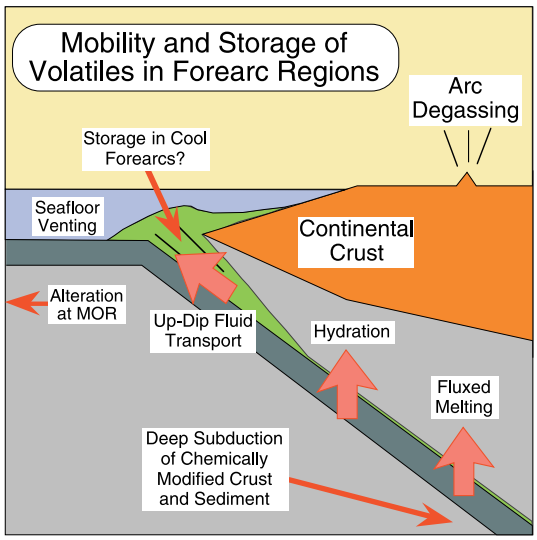

Figure 1. Schematic illustration of a subduction zone showing some of the possible fluxes of volatile and fluid-mobile trace elements. Large quantities of sedimentary rocks and seafloor-altered basalt, containing abundant volatile elements, are delivered to subduction zones. Most pore water is lost as the rocks are subducted through the upper 5–10 kilometers [*Moore et al.*, 1990]. However, some fraction of the volatile elements must be retained to participate in up-dip fluid transport [*Vrolijk et al.*, 1990; *Benton*, 1997; *Benton et al.*, 2001], hydration of the mantle wedge [*Peacock*, 1993; *Fryer et al.*, 1999], arc volcanism [*Morris et al.*, 1990], and potentially, addition to the deep mantle of surficially derived volatile elements [*Cartigny et al.*, 1998].

Coast Ranges, Franciscan Complex peak metamorphic P-T conditions range from <0.3 GPa and ~100°C in the Coastal Belt to ~300°C and 0.8–0.9 GPa in the Eastern Belt, based on vitrinite reflectance and the presence or absence of high-P indicator minerals (see summary by *Blake et al.* [1987]; see Figure 3). In the Pacheco Pass area (Diablo Range, California) peak pressures are thought to have been ~0.7–0.8 GPa, peak-T estimates are 200 ± 50°C (see recent data and summaries of earlier data in *Ernst* [1993] and *Dalla Torre et al.* [1996]). The Western Baja Terrane (WBT) is divided into three subterranes that have experienced peak P-T conditions of >0.8 GPa and 225–235°C (ST-1), ~0.7–0.8 GPa and 170–220°C (ST-2) and ~0.5–0.6 GPa and 175–200°C (ST-3; *Sedlock* [1988]; see Figure 3).

[5] Sampling locations from the Coast Ranges for which data are presented in this paper are shown on Figure 2, a table with coordinates of these localities is included in appendix A. Where possible, relatively areally extensive outcrops were examined in order to observe veining styles, textures, and vein-host rock relations (discussion of fluid mobility in *Sadofsky and Bebout* [2001a]). Additional outcrops were analyzed in the Pacheco Pass area of the Diablo Range in central California. Samples of the Western Baja Terrane from Cedros Island were provided by R. Sedlock, and sample localities correspond to those of *Sedlock* [1988].

[6] Field locations differ significantly in lithology among the major belts of the Coast Ranges (Coastal, Central and Eastern Belts) and the units of the Diablo Range. Rocks in the Coastal Belt appear only mildly metamorphosed and they are composed primarily of greywacke that varies in scale of interbedding from several centimeters to several tens of meters. The greywacke generally occurs as lenticular blocks surrounded by a more deformed shale matrix. The greywackes preserve abundant brittle deformation features, such as veins in cracks, whereas the shale matrix appears to deform more ductily. These greywackes of the Coastal Belt are dominated by clastic grains of quartz, feldspars, clays, and opaques, with other minor detrital grains and lithic fragments. Prograde minerals such as minor white mica (mainly as sericitization of feldspar), laumontite (mainly in veins), chlorite, and calcite are also commonly present (see Table 1 for summary of mineralogy). Trace minerals include zircon, apatite, and tourmaline.

[7] The Central Belt has a macroscopic texture characterized as blocks in mélange [see *Cloos*, 1986] and, like the Coastal Belt, coarser greywackes preserve many more brittle deformation features than the shale matrix. Metasedimentary rocks from the Central Belt retain some detrital grains (like those the Coastal Belt), but there is a greater degree of recrystallization in the Central Belt. Fewer lithic clasts remain, and those that do are more altered than in the Coastal Belt. These rocks differ from the Coastal Belt in several ways: there are fewer clays present; and much more white mica, lawsonite, and pumpellyite; most calcite has been transformed into aragonite [*Terabayashi and Maruyama*, 1998]; most detrital

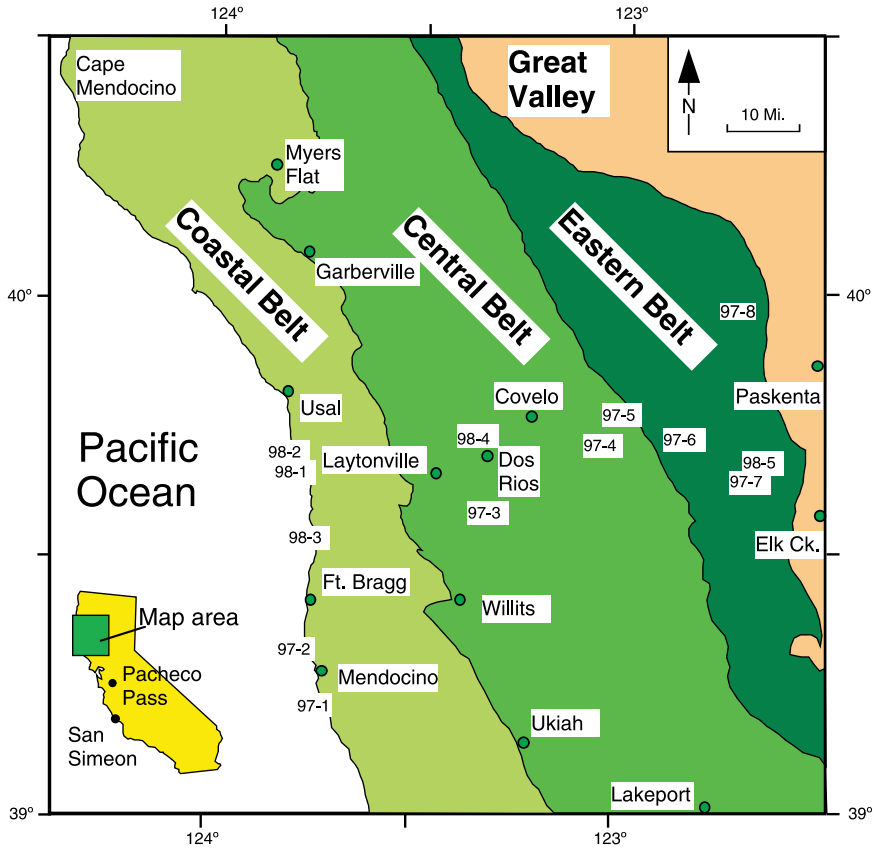

Figure 2. Map of the Coast Ranges showing the locations of analyzed samples and their relations to the main lithotectonic subdivisions of the Franciscan Complex, after *Blake et al.* [1987]. Numbers represent sample sites from the northern Coast Ranges.

K-feldspar has been replaced by albite [see *Blake et al.*, 1987] (Table 1). Other minerals commonly present in Central Belt samples include stilpnomelane, apatite, epidote, sodic amphibole, titanite, and opaques.

[8] The Eastern Belt rocks show a much stronger metamorphic texture and contain more high-P indicator minerals, such as lawsonite, sodic amphibole, and sodic pyroxene, and no remaining detrital K-feldspar (see textural zones of *Blake et al.* [1987] and *Jayko and Blake* [1989]). Cleavage is very well developed in the more pelitic rocks, and some outcrops show development of segregation textures. Samples analyzed in this study are primarily composed of quartz, albite, white-mica (phengite and paragonite [*Jayko et al.*, 1986]), lawsonite, stilpnomelane, and pumpellyite, with relatively minor epidote, titanite, and zircon. Other phases include sodic pyroxene, sodic amphibole, chlorite, tourmaline, and apatite [*Blake et al.*, 1987; *Tagami and Dumitru*, 1996].

[9] Samples analyzed from the Pacheco Pass area are composed primarily of quartz, albite, sodic pyroxene, white-mica, and lawsonite, with more minor occurrences of chlorite, carbonate, titanite, sodic amphibole, stilpnomelane, zircon, and prehnite (see Table 1). Other mineral phases present include pumpellyite and calcite or aragonite. Abundant mineral-chemical study has provided a solid understanding of the P-T history of these rocks, which are probably the most deeply subducted intact tract of metasedimentary rocks in the Franciscan Complex [*Ernst*, 1993].

[10] Cedros Island, Baja California, hosts outcrops of seafloor sediments and mafic rocks metamorphosed to blueschist-facies conditions during Early Cretaceous subduction [*Sedlock*, 1988, 1996; *Baldwin and Harrison*, 1989, 1992]. Metasedimentary

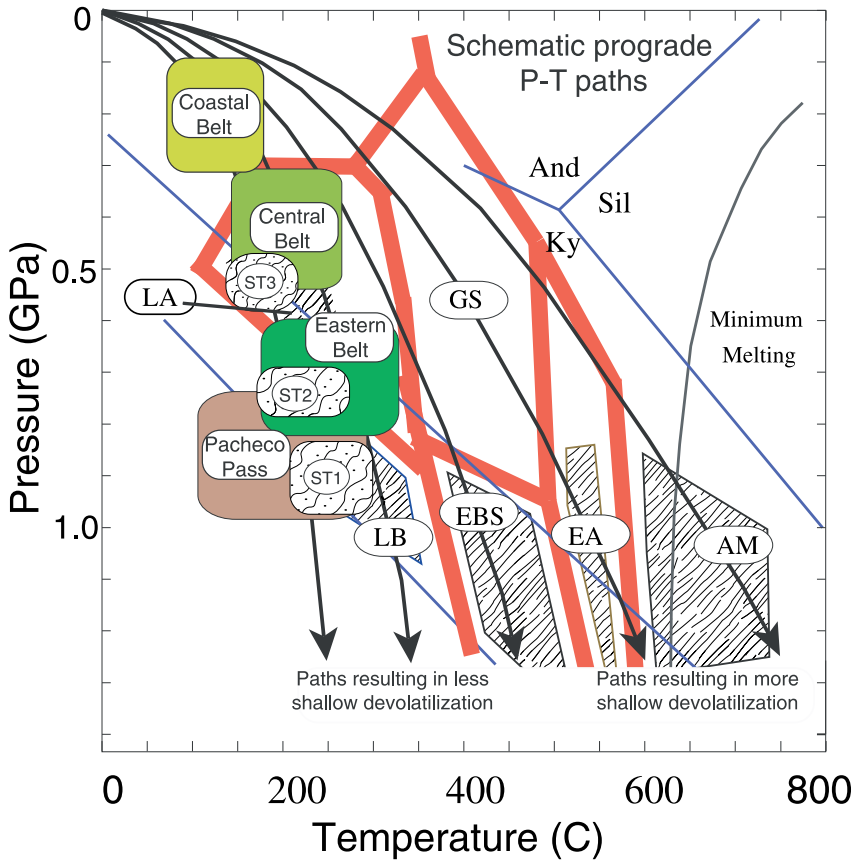

Figure 3. Pressure-temperature diagram showing estimates of peak metamorphic recrystallization of each of the Franciscan units studied here and the subterranes of the Catalina Schist (exposed on Santa Catalina Island, California). P-T estimates from *Blake et al.* [1987]; *Sedlock* [1988]; *Jayko and Blake* [1989]; *Ernst* [1993]; *Grove and Bebout* [1995]; *Dalla Torre et al.* [1996]; and *Tagami and Dumitru* [1996]; *Terabayashi et al.* [1996]. Generalized phase equilibria for relevant volcanic and volcaniclastic rocks from *Liou et al.* [1987], *Evans* [1980], and *Frey et al.* [1991].

rocks analyzed in this study, from all three of the subterranes of the Western Baja Terrane (ST-1, ST-2, and ST-3; after *Sedlock* [1988]), show varying grain sizes and sand:shale ratios. Metasedimentary rocks from ST-1 are composed primarily of quartz + jadeite + lawsonite ± crossite-glaucophane ± chlorite ± white mica, and oxide minerals and reduced-C are also present. Veins primarily contain quartz, albite, calcite/aragonite, but occasionally contain other high-P phases (sodic pyroxene, sodic amphibole). Peak P-T conditions estimated for this unit are >0.8 GPa and 225–325°C [*Sedlock*, 1988]. Subterrane-2 is composed of a slightly lower-T and lower-P assemblage (0.7–0.8 GPa, 170–220°C), and contains significant albite, less jadeite, and more lawsonite than ST-1 samples. Samples rom ST-3 record peak conditions lower in P than ST-1 and ST-2, with most rocks containing the metamorphic assemblage of quartz + albite ± epidote + lawsonite. Estimates of peak conditions are 0.5–0.6 GPa and 175–200°C [*Sedlock*, 1988] (Figure 3).

3. Analytical Methods

[11] Samples for major and trace element whole-rock geochemical analyses were prepared by first removing any obvious weathering rind, then washing in deionized water and powdering in an alumina mortar and pestle. Most analyses were performed by Activation Laboratories Inc. (Ancaster, Ontario, Canada). Major element oxides and Ba, Sr, and Y

Table 1. Mineralogy of Samples Analyzed From the Franciscan Complex

Site	Sample	Qtz	Fsp	Mica	Chl	L.F.	CO_3	Clay	Lw	Ttn	Gln	Jd	Ep	Stp	Pmp	Other
Coast Ranges-Coastal																
97-1	VD-2A	x	K + Pl	W	x	x	x	x	-	-	-	-	-	-	-	Zr
97-1	VD 5c	x	K + Pl	Bt	x	x	x	x	-	-	-	-	-	-	-	Ap
97-1	VD-9B	x	K + Pl	Bt	x	x	x	x	-	-	-	-	-	-	-	Lm
97-2	Mendo 8	x	K + Pl	-	x	x	x	x	-	-	-	-	-	-	-	
97-2	Mendo 4	x	K + Pl	-	x	x	x	x	-	-	-	-	-	-	-	Tour, Lm
98-1	KW98-1	x	Ksp	W + Bt	x	x	x	x	-	x	-	-	-	-	-	Lm, detrital Ol
98-1	KW98-14a	x	K + Pl	W + Bt	x	x	x	x	-	-	-	-	-	-	-	Zr
98-1	KW98-21a	x	K + Pl	W + Bt	x	x	x	x	-	-	-	-	-	-	-	
98-1	KW98-21b	x	K + Pl	W + Bt	x	x	x	x	-	x	-	-	-	-	-	Lm, detrital Ol
98-2	KW98-52	x	Ksp	Bt	x	x	x	x	-	x	-	-	-	-	-	
98-3	KW98-91	x	K + Pl	Bt		x	x	x	-	-	-	-	-	-	-	
98-3	KW98-93	x	K + Pl	Bt	x	x	x	x	-	-	-	-	-	-	-	
Coast Ranges-Central																
97-3	EEL4SH	x	Ab	W	-	x	x	-	-	-	-	-	tr	x	x	Ap
97-3	EEL4GW	x	Ab	W	-	x	x	-	x	-	-	-	tr	x	x	Lm
97-4	JC-4	x	x	W	x	x	x	-	x	-	-	-	-	-	x	
97-4	JC c4a	x	x	W	x	x	x	-	x	-	-	-	-	-	-	
97-4	JC-5	x	Ab	W	x	-	x	x	x	tr	-	-	tr	-	-	
97-4	JC 6	x	-	W	x	-	-	x	x	-	tr	-	tr	-	-	
98-4	P&S 2a	x	-	W	-	-	-	-	x	x	tr	-	-	-	-	
97-5	APC5A	x	Ab	W	-	Bt	-	-	x	-	tr	-	-	-	x	
97-5	APc5b	x	Ab	W	-	Bt	-	-	x	tr	-	-	-	-	-	
97-5	AP8-6	x	Ab	W	x	Bt	x	-	x	-	tr	-	-	-	x	
Coast Ranges-Eastern																
97-6	CR-2B	x	-	W	-	-	-	-	-	-	-	-	-	x	-	Tour
98-5	AS2-B	x	-	W	-	-	-	-	-	-	-	-	tr	-	x	
97-7	Alder 1c	x	Ab	W	-	-	-	-	x	-	-	-	-	x	-	
97-7	Alder 2	x	-	W	-	-	-	-	x	-	-	-	tr	x	-	
97-7	Alder 4b2	x	Ab	W	-	-	-	-	x	-	-	-	-	x	-	
98-5	AS2-b	x	Ab	W	-	-	-	-	-	-	-	-	tr	x	x	
97-8	T4	x	-	W	-	-	-	-	x	x	-	-	-	x	x	
97-8	T8	x	Ab	W	-	-	-	-	-	x	-	-	-	x	x	
Pacheco Pass Area																
	EP4	x	Ab	W	-	-	-	-	x	-	-	x	-	-	-	Zr
	EP6	x	Ab	-	-	-	-	-	x	x	-	-	-	-	-	Zr
	WGE-Q20	x	Ab	W	x	-	-	-	x	x	-	x	-	-	-	Prh, Zr
	WGE-Q26f	x	-	-	-	-	-	-	x	x	x	x	-	x	-	
	WGE-Q26g	x	-	-	-	-	-	-	x	x	x	x	-	-	-	
	WGE-Q34	x	-	W	x	-	x	-	x	x	x	x	-	-	-	
	WGE-Q38	x	Ab	x	x	-	x	-	x	-	-	x	-	-	-	
Western Baja Terrane																
	ST-1	x	±Ab	±	±				x		±	x				
	ST-2	x	Ab		±				±		±	±				
	ST-3	x	Ab						±				±			

were analyzed by inductively coupled plasma techniques (ICP). Other trace elements were analyzed by ICP-MS following fluxed fusions (Zr, Cs, Ce, Nd, Eu, Gd, Tb, Dy, Ho, Er, Tm, Yb, Lu, Hf, Ta, Th, and U), pressed pellet X-ray fluorescence (Nb, Rb, Pb, S), and induced neutron activation analysis (As, Sb, La, and Sm). Boron concentrations were analyzed at the University of South Florida by direct current plasma emission spectrometry (methods described by *Ryan and Langmuir* [1993]). Loss-on-ignition (LOI) was determined by weight loss resulting from heating for 2 hours at 1050°C.

[12] For stable-isotope analyses, clean, unweathered rock samples (approximately 0.25 kg) were crushed in a jaw crusher and then in a disk mill to a size of <1 mm. Nitrogen isotopic composition was

Table 2. Major Element Compositions Of Franciscan and WBT Samples[a]

Site	Sample	SiO_2	Al_2O_3	Fe_2O_3	MnO	MgO	CaO	Na_2O	K_2O	TiO_2	P_2O_5	LOI
Coast Ranges-Coastal												
97-1	VD-2A	60.15	19.87	7.25	0.06	3.58	1.57	2.10	4.16	0.91	0.36	5.98
97-1	VD-9B	68.56	14.21	5.15	0.07	2.05	3.23	3.48	2.52	0.56	0.17	3.66
98-1	KW98-21B	67.23	13.98	3.34	0.10	1.49	7.63	3.50	1.92	0.66	0.16	6.32
98-1	KW98-1	67.55	13.91	2.27	0.11	1.02	8.78	3.70	2.13	0.42	0.11	7.05
Coast Ranges-Central												
97-3	EEL4SH	47.09	13.69	7.97	0.10	3.81	13.76	1.62	2.33	0.58	9.06	6.17
97-3	EEL4GW	68.03	14.94	5.70	0.08	2.91	2.19	3.34	2.03	0.63	0.14	3.72
97-4	JC-4	70.76	14.23	4.02	0.07	2.27	1.76	4.42	1.90	0.47	0.10	2.56
97-4	JC-5	68.01	15.83	5.34	0.10	2.85	1.83	3.81	1.41	0.73	0.08	4.01
97-5	APC5A	71.55	13.82	4.57	0.06	2.56	1.12	4.61	1.02	0.55	0.14	2.45
97-5	AP8-6	62.30	18.39	7.73	0.14	3.16	4.13	1.12	2.14	0.73	0.16	7.20
Coast Ranges-Eastern												
97-6	CR-2B	74.21	12.91	4.57	0.05	2.14	0.77	3.26	1.31	0.57	0.22	3.08
98-5	AS2-B	66.19	14.96	7.40	0.10	3.61	0.95	4.38	1.34	0.73	0.36	2.71
97-7	ALDER2	68.60	15.19	7.22	0.08	2.96	0.39	3.49	1.14	0.66	0.27	3.07
97-8	T4	68.14	15.31	7.27	0.10	3.36	0.82	2.20	1.89	0.71	0.20	3.78
97-8	T8	66.56	17.12	7.02	0.10	3.34	0.54	1.39	2.93	0.81	0.19	5.66
Pacheco Pass Area												
	EP4	58.30	18.84	7.33	0.07	7.47	0.30	3.01	3.48	0.96	0.22	7.20
	EP6	70.61	14.90	4.74	0.05	2.22	1.50	3.22	1.92	0.62	0.23	3.42
	Q26F	68.94	14.09	4.45	0.05	2.45	4.42	4.34	0.37	0.70	0.20	3.94
	Q38	71.43	14.02	4.54	0.07	2.31	2.17	3.31	1.50	0.56	0.10	3.12
Western Baja Terrane-ST1												
	585-1	63.63	14.13	6.78	0.10	3.20	7.78	2.59	1.10	0.55	0.15	7.12
	585-14	63.13	15.66	7.99	0.16	4.35	2.21	3.86	1.52	0.86	0.27	4.61
	585-83A	76.38	11.84	2.78	0.08	1.21	3.84	2.37	0.93	0.42	0.15	3.21
	585-14B	77.32	11.89	2.89	0.03	1.34	0.60	4.09	1.10	0.64	0.10	2.11
Western Baja Terrane-ST2												
	585-138	68.51	14.90	5.71	0.09	2.32	1.37	4.88	1.26	0.77	0.18	2.95
	486-105	68.53	14.26	4.39	0.11	4.60	0.72	3.38	3.24	0.66	0.11	3.29
	585-71	75.08	12.00	5.41	0.08	1.80	0.47	3.55	0.85	0.57	0.19	2.56
Western Baja Terrane-ST3												
	585-133	65.80	15.34	6.80	0.15	3.05	1.21	6.33	0.47	0.71	0.15	3.05
	585-121	65.27	15.11	7.04	0.11	3.46	1.38	5.95	0.47	1.06	0.16	2.80
	585-179	66.17	16.46	5.15	0.10	1.77	3.51	4.48	1.46	0.80	0.10	2.63
	486-130	76.67	11.90	3.06	0.04	1.08	2.27	3.54	0.93	0.42	0.10	2.36
Standards analyzed with these samples												
	SY-3 syenite	60.66	11.75	6.55	0.328	2.62	8.27	4.14	4.48	0.143	0.55	
	MRG-1 gabbro	38.40	8.48	17.71	0.167	13.35	14.21	0.73	0.19	3.827	0.08	
	USGS W-2	53.03	15.31	10.94	0.168	6.39	10.89	2.19	0.58	1.067	0.14	
	USGS DNC-1	47.04	18.42	9.93	0.147	10.08	11.15	1.88	0.22	0.472	0.06	
	USGS BIR-1	48.63	15.72	11.07	0.174	9.75	13.36	1.79	0.04	0.952	0.02	
	USGS G-2	67.85	15.33	2.70	0.034	0.74	1.96	4.17	4.55	0.477	0.14	
	NBS 1633a	48.88	26.61	13.33	0.021	0.74	1.56	0.22	1.88	1.366	0.38	
	USGS STM-1	62.12	18.28	5.36	0.226	0.10	1.17	8.89	4.21	0.128	0.17	
	CRPG IF-G	40.12	0.16	55.85	0.036	1.93	1.50	0.06	0.05	0.004	0.06	
	CRPG AC-E	69.46	14.45	2.59	0.057	0.02	0.35	6.48	4.40	0.098	0.02	

[a] Note-Major oxides are normalized to 100% without LOI.

analyzed by sealed-tube combustion (910°C for 4 hours; see discussion of N-isotope techniques in *Bebout and Fogel* [1992], *Sadofsky and Bebout* [2000], and *Bebout and Sadofsky* [2003]). For reduced-C analyses of $\delta^{13}C$, samples were reacted overnight in 10 ml of 1N HCl to remove any carbonates. The samples were then centrifuged and rinsed three times to remove all HCl, then dried and finally prepared for isotopic analysis by sealed-tube combustion (850°C for 1.5 hours). Concentrations of C were determined by Hg manometry after cryogenic purification of the resulting CO_2. CO_2 from carbonate cements was prepared by dissolution in 100% phosphoric acid at 25°C

Table 3 (Representative Sample). Concentrations of Selected Trace Elements From the Franciscan Complex and WBT [The full Table 3 is available in the HTML version of this article at http://www.g-cubed.org]

Site	Sample	La	Ce	Pr	Nd	Sm	Eu	Gd	Tb	Dy	Ho	Er	Tm	Yb	B	Cs	Rb	Ba	Th	U	Nb	Ta	Sr	Pb	Lu	Hf
Coast Ranges-Coastal																										
97-1	VD-2A	32.2	63.1	8.15	31.5	6.26	1.67	6.16	0.96	5.33	1.08	3.16	0.488	3.27	20.6	14.5	166	531	9.22	3.01	11.2	0.8	198	24	0.483	4.6
97-1	VD-9B	25.4	46.5	5.91	21.9	4.34	1.14	4.06	0.60	3.37	0.69	2.07	0.318	2.22	8.0	2.6	81	939	7.57	2.37	10.7	0.7	282	14	0.322	4.1
98-1	KW98-21B	32.6	58.5	7.33	26.9	5.09	1.30	4.71	0.70	3.95	0.77	2.31	0.375	2.52	7.2	1.9	72	904	9.09	2.65	12.5	1.0	372	22	0.378	6.3
98-1	KW98-1	21.3	37.3	4.77	17.9	3.47	1.11	3.24	0.48	2.61	0.52	1.55	0.229	1.60	12.7	2.1	78	896	5.64	1.72	8.6	0.6	414	11	0.239	3.2
Coast Ranges-Central																										
97-3	EEL4SH	32.6	55.9	6.74	23.5	4.25	1.01	3.89	0.59	3.30	0.67	1.92	0.307	2.03	19.3	5.8	101	376	5.19	1.85	7.9	0.5	268	16	0.381	0.5
97-3	EEL4GW	16.0	29.3	3.81	14.3	3.04	0.846	2.87	0.48	2.78	0.57	1.69	0.263	1.79	4.5	3.1	77	275	7.25	2.44	10.9	0.7	116	15	0.29	4.4
97-4	JC-4	31.4	44.6	5.64	22.8	4.78	2.08	5.44	0.80	4.45	0.91	2.57	0.373	2.50	6	3.2	90	338	10.7	3.52	14.2	1.1	116	18	0.286	3.9
97-4	JC-5	24.1	42.9	5.48	20.0	3.94	1.09	3.89	0.60	3.29	0.67	1.99	0.310	2.02	4.6	3.9	54	407	5.74	2.22	7.1	0.5	100	11	0.27	3.8
97-5	APC5A	26.6	51.3	6.46	24.2	5.11	1.40	4.96	0.83	4.65	0.92	2.74	0.414	2.82	12.2	2.2	39	311	5.27	1.86	8.3	0.6	81	14	0.271	3.0
97-5	AP8-6	11.1	19.5	2.57	10.0	2.53	0.837	2.76	0.46	2.75	0.57	1.71	0.253	1.72	9.3	4.5	74	956	9.61	3.50	13.2	1.0	351	23	0.405	4.0
Coast Ranges-Eastern																										
97-6	CR-2B	18.8	34.4	4.44	17.0	3.50	1.01	3.40	0.57	3.24	0.67	2.01	0.317	2.08	4.3	2.4	44	487	3.42	1.22	5.8	0.4	36	14	0.248	2.8
98-5	AS2-B	7.92	15.1	2.08	8.78	2.44	0.600	2.54	0.44	2.58	0.55	1.66	0.280	1.87	8.8	1.8	48	382	4.74	1.65	7.8	0.5	40	15	0.314	3.5
97-7	ALDER2	14.7	30.8	3.84	15.1	3.36	0.913	3.41	0.57	3.21	0.66	2.00	0.305	2.09	1.6	2.6	48	417	4.08	1.68	7.5	0.5	24	12	0.279	3.1
97-8	T4	17.7	34.8	4.58	17.7	3.88	0.975	3.93	0.64	3.69	0.76	2.35	0.376	2.55	16.2	3.3	64	761	4.52	1.32	7.5	0.5	31	9	0.312	2.9
97-8	T8	28.2	48.6	5.36	17.5	2.74	0.689	2.95	0.44	2.61	0.63	2.12	0.359	2.48	43.5	5.0	86	1751	5.09	1.83	7.6	0.6	78	22	0.375	3.3
Pacheco Pass Area																										
	EP4	27.6	46.7	5.72	20.3	3.59	0.995	3.47	0.51	2.91	0.62	1.86	0.290	2.05	1.8	8.9	125	735	8.64	2.30	12.3	0.8	40	21	0.401	4.7
	EP6	13.1	25.5	3.75	15.7	3.79	1.09	3.77	0.65	3.83	0.79	2.32	0.356	2.36	5.0	3.5	83	631	6.56	2.27	9.5	0.7	87	22	0.308	3.2
	Q38	7.38	14.3	2.10	9.07	2.25	0.821	2.51	0.46	2.80	0.61	1.83	0.286	1.89	7.5	2.2	58	454	7.71	2.06	8.6	0.7	108	11	0.316	4.6
Western Baja Terrane-ST1																										
	585-1	21.3	41.5	5.63	22.1	4.89	1.42	4.89	0.84	4.77	0.95	2.70	0.394	2.67	4.5	2.0	35	338	1.11	0.45	2.0		284	7	0.271	1.4
	585-14	12.7	22.9	3.01	11.5	2.42	0.791	2.38	0.41	2.43	0.50	1.56	0.238	1.59	1.8	3.8	65	384	5.77	1.89	7.7	0.5	99	15	0.383	4.5
	585-83A	11.9	21.2	2.74	10.1	1.90	0.522	1.85	0.31	1.83	0.37	1.17	0.190	1.27	1.6	1.4	29	228	3.50	1.24	3.5	0.3	243	11	0.226	2.0
	585-14B	15.1	29.7	4.22	16.9	3.76	1.05	3.97	0.68	4.07	0.84	2.49	0.392	2.60	4.7	2.3	50	354	4.60	1.54	9.4	0.6	55	12	0.19	2.8
Western Baja Terrane-ST2																										
	585-138	21.2	39.7	5.33	19.9	3.79	0.762	3.39	0.59	3.45	0.69	2.09	0.347	2.28	4.6	1.7	51	194	4.58	1.37	6.2	0.4	101	11	0.378	3.6
	486-105	10.2	19.5	2.57	9.82	2.09	0.472	1.99	0.34	2.03	0.41	1.23	0.201	1.37	1.9	3.3	106	226	7.52	1.90	6.5	0.5	22	8	0.328	4.6
	585-71	9.22	18.2	2.60	10.8	2.60	0.866	2.71	0.49	2.82	0.58	1.78	0.270	1.84	11.6	1.7	36	301	4.54	1.56	6.8	0.5	34	21	0.203	3.7
Western Baja Terrane-ST3																										
	585-133	15.4	29.3	4.14	17.1	3.87	1.14	3.90	0.70	4.21	0.86	2.57	0.403	2.67	7.5	0.7	13	163	2.26	0.87	3.4	0.2	72	8	0.257	2.2
	585-121	20.5	38.3	5.17	20.0	4.38	1.20	4.44	0.76	4.50	0.95	2.83	0.448	2.96	3.9	0.6	15	254	3.35	1.35	5.4	0.4	83	1	0.394	4.2
																								1		
	585-179	19.2	34.6	4.44	16.3	3.28	0.871	3.18	0.52	3.04	0.62	1.82	0.287	1.79	12.1	1.7	55	450	6.85	1.79	7.2	0.5	152	9	0.437	5.7
	486-130	20.8	35.6	4.48	16.2	3.15	0.872	2.98	0.50	2.92	0.59	1.77	0.275	1.83	7.9	1.4	35	305	5.32	1.17	4.2	0.4	180	13	0.266	3.5
Standard Data																										
Blank			−0.1	−0.1	−0.02	−0.05	−0.02	−0.005	−0.02	−0.01	−0.02	−0.01	−0.01	−0.01	−0.01		−0.1	−2		−0.05	−0.05	−0.5	−0.1		−10.002	−0.1
Standard MAG1	43.4		86.6	10.3	37.0	7.04	1.50	5.98	0.94	5.21	0.99	2.93	0.40	2.69		8.6	144		11.2	2.60	13.3	1.2		0.379	3.3	126

Geochemistry Geophysics Geosystems G3
SADOFSKY AND BEBOUT: FOREARC DEVOLATILIZATION 10.1029/2002GC000412

overnight, then purified and measured in the same manner as CO_2 from the reduced-C experiments. All gases were analyzed for isotopic composition on a Finnigan MAT 252 mass spectrometer at Lehigh University, and isotopic compositions are presented as $\delta^{13}C_{VPDB}$, $\delta^{15}N_{air}$ and $\delta^{18}O_{VSMOW}$. Uncertainties, determined by replicates of internal and international standards, are $\leq$0.10‰ (1σ) for all isotope analyses.

4. Results

[13] Thirty metasedimentary samples were analyzed for whole-rock major- and trace-element compositions. These data are presented in Tables 2 and 3 and briefly introduced in this section. SiO_2/Al_2O_3 (regarded as a rough measure of sandstone/shale lithologic proportions; *Cullers*, 2000) ranges from 3.0 to 6.5 in the rocks in this study, with most rocks containing ~60–75 wt.% SiO_2 and 12–18 wt.% Al_2O_3 (Figure 4). K_2O concentration ranges from 0.37 wt.% in one very quartz-rich rock to 4.16 wt.% in the most pelitic rock of this study and shows a crude negative correlation with SiO_2/Al_2O_3 (Figure 5a). Na_2O concentration is more variable than K_2O concentration and does not appear to correlate as well with SiO_2/Al_2O_3 ratio for the metasedimentary suites analyzed in this study (Figure 5b). Loss-on-ignition (LOI) ranges from 2.11 to 7.20 wt.% (Table 2a) and appears to anticorrelate weakly with SiO_2/Al_2O_3 (Figure 6). Rare earth element (REE) patterns, normalized to chondritic values, show LREE enrichments and are broadly similar to both the average compositions of subducted sediment [*Plank and Langmuir*, 1998] (GLOSS composite) and continental arc turbidites [*McLennan*, 1990] (Figure 7). Alkali elements and B are highly variable in concentration correlating at least crudely with sandstone/shale indicators such as K_2O content (13–166 ppm Rb; 0.5–14.5 ppm Cs; and 1.6–43.5 ppm B; Figure 8).

[14] Forty-one whole-rock metasedimentary samples were analyzed for the concentration and $\delta^{13}C$ of carbon present in its reduced form as graphite or partially metamorphosed organic detritus (Table 4, Figure 9). Reduced C content ranges from 0.02 wt.% in some of the more siliceous rocks to > 1.2 wt.% in fine-grained, more aluminous metasedimentary rocks, and the reduced-C $\delta^{13}C$ of the same samples ranges from −28.8 to −21.9‰. In the Coast Ranges, Coastal Belt metagreywackes range from 0.13 to 0.89 wt.% C with $\delta^{13}C$ = −25.4 to −24.9‰, showing the most uniformity in C compositions (see field on Figure 9). In the Central Belt, C content ranges from <0.1 to >1 wt.% with a slightly wider range in $\delta^{13}C$ (−28.2 to −24.1‰). Eastern Belt metasedimentary rocks contain similar quantities of C (0.1 to 1.0 wt.%) with a range in $\delta^{13}C$ (−27.2 to

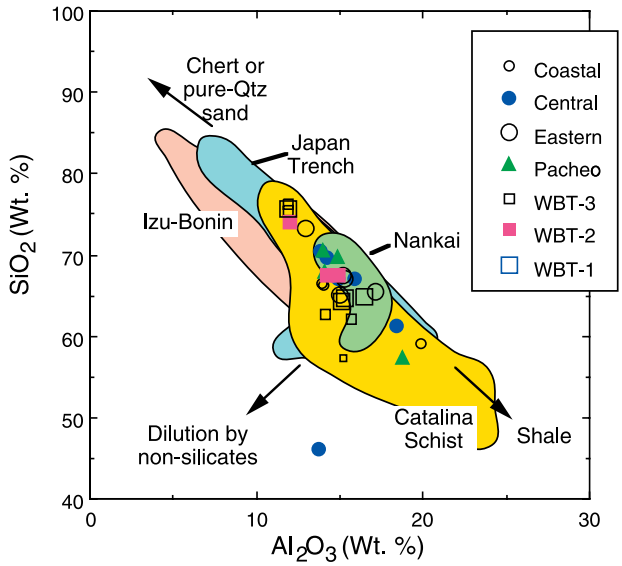

Figure 4. Concentrations of SiO_2 and Al_2O_3 show the relative proportions of sand and clay in the samples. Data plotted here are corrected for loss on ignition in order to compare the lithological variations of both sedimentary protoliths and high-grade metamorphic rocks such as the Catalina Schist. Values from this study are broken down by lithotectonic sub-unit and data presented from the literature are from the following references: Japan Trench—sediments recovered by DSDP legs 56 and 57 on the subducting Pacific Plate [*Murdmaa et al.*, 1980]; Catalina—metasedimentary samples of the Catalina Schist [*Bebout et al.*, 1999]; Sambagawa—metasediments of the Sambagawa Belt [*Nakano and Nakamura*, 2001]; Nankai—clastic sediments of the Nankai Trough [*Pickering et al.*, 1993]; and Izu-Bonin—clastic sediments from ODP leg 185, site 1149A. This figure shows the general linear array of all greywackes in SiO_2-Al_2O_3 space, with some extremes of high SiO_2 due to mixing with siliceous oozes and extremes of Al_2O_3 in some of the extremely pelitic rocks of the Catalina Schist. Departures from the linear array of SiO_2 vs. Al_2O_3 can be caused by dilution by non-silicate phases such as calcite or apatite.

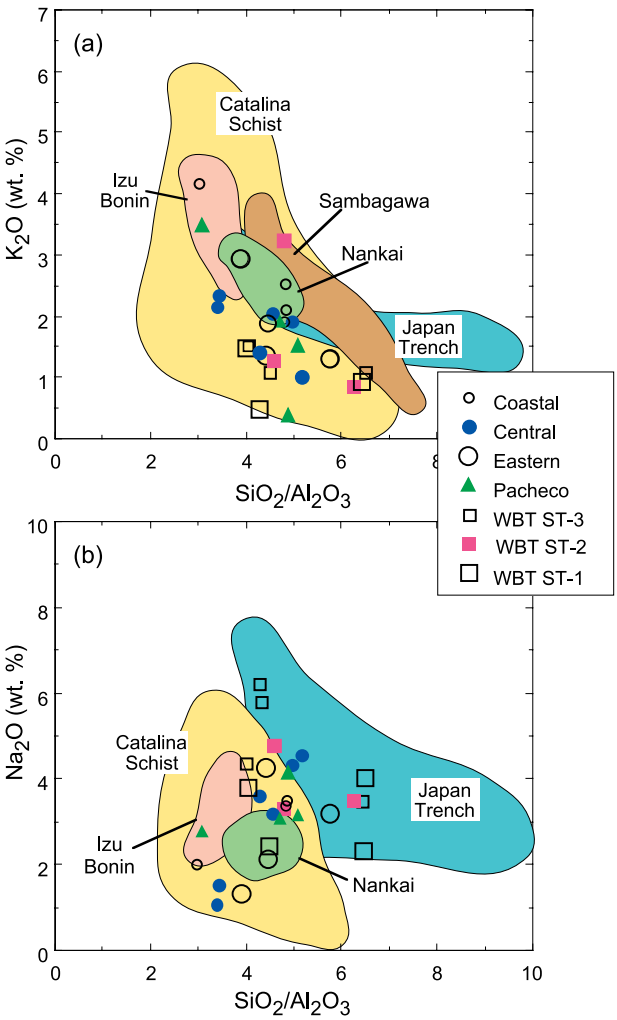

Figure 5. Because of the near linear SiO_2-Al_2O_3 relationships, the ratio of SiO_2 to Al_2O_3 is used as a proxy for the relative proportions of sand to shale. K_2O variations (a) show a strong correlation with sandstone/shale relations. Na_2O (b) does not correlate as well with SiO_2/Al_2O_3 because there are many processes that may control the Na_2O concentration of the sedimentary protoliths.

−23.8‰) similar to that of the Central Belt. One mafic sample from the Eastern Belt contains 0.02 wt.% reduced C with $\delta^{13}C = -25.9$‰. Samples from the Pacheco Pass area and the Western Baja Terrane generally contain less reduced C than samples of the Coast Ranges (Pacheco Pass samples contain 0.04 to 0.23 wt.%, and WBT samples contain 0.06 to 0.37 wt.%). Samples from the Pacheco Pass area have $\delta^{13}C$ (−26.8 to −24.2‰) similar to those of samples from the Coast Ranges, and rocks from the Western Baja Terrane show a much wider range of $\delta^{13}C$ (−28.8 to −21.9‰). Concentration and C- and O-isotopic compositions of finely disseminated calcite (presumably relict cements; see *Bebout* [1991]) were analyzed for a subset of eleven of the lower-grade samples. These analyses were undertaken only for the lower-grade samples of the Coastal and Central Belts because calcite cement was not observed petrographically in the higher-grade rocks. Calcite concentrations vary from nearly absent to ∼12 wt.%, and $\delta^{13}C$ (−13 to 0‰) and $\delta^{18}O$ (+12.8 to +17.3‰) values are similar to those of veins in these rocks (see discussions of veins and fluid mobility by *Sadofsky and Bebout* [2001a]).

[15] Thirty metasedimentary whole-rock samples were analyzed for N concentration and $\delta^{15}N$ (Table 4, Figure 10). Nitrogen concentration ranges from 102−891 ppm and $\delta^{15}N$ ranges from +0.1 to +3.0‰. Coastal Belt (Coast Ranges) metagreywackes (representing the shallowest subduction) contain 102 to 891 ppm N with $\delta^{15}N$ = +1.4 to +3.0‰, and N contents and $\delta^{15}N$ crudely covary

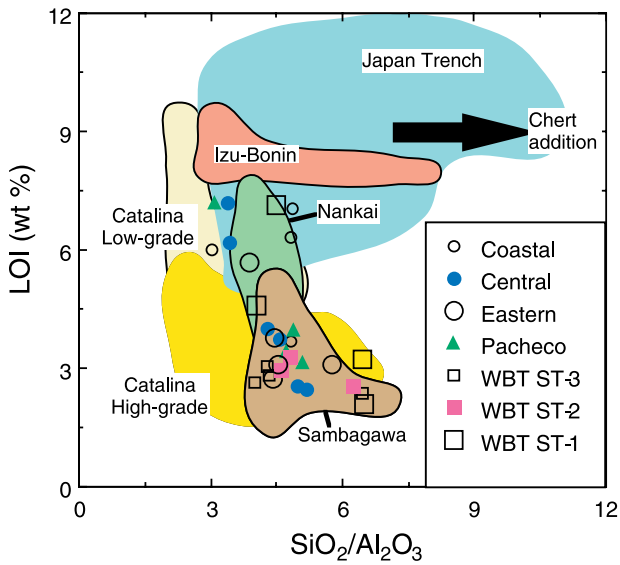

Figure 6. Loss on ignition (LOI) correlates well with SiO_2/Al_2O_3 for the data from this study and is similar to other subduction-zone metamorphic suites such as the Catalina Schist and the Sambagawa belt. Samples from the Catalina Schist are broken down into Low-grade (lawsonite-albite and lawsonite blueschist facies) and high-grade (epidote-blueschist to amphibolite facies). Representative marine sediments have LOI vs SiO_2/Al_2O_3 relationships that appear to commonly be somewhat higher in LOI than the samples from this study and other metamorphosed sediments. The extremely high-LOI high SiO_2/Al_2O_3 samples are probably due to dilution of the greywacke signal by pelagic silica oozes.

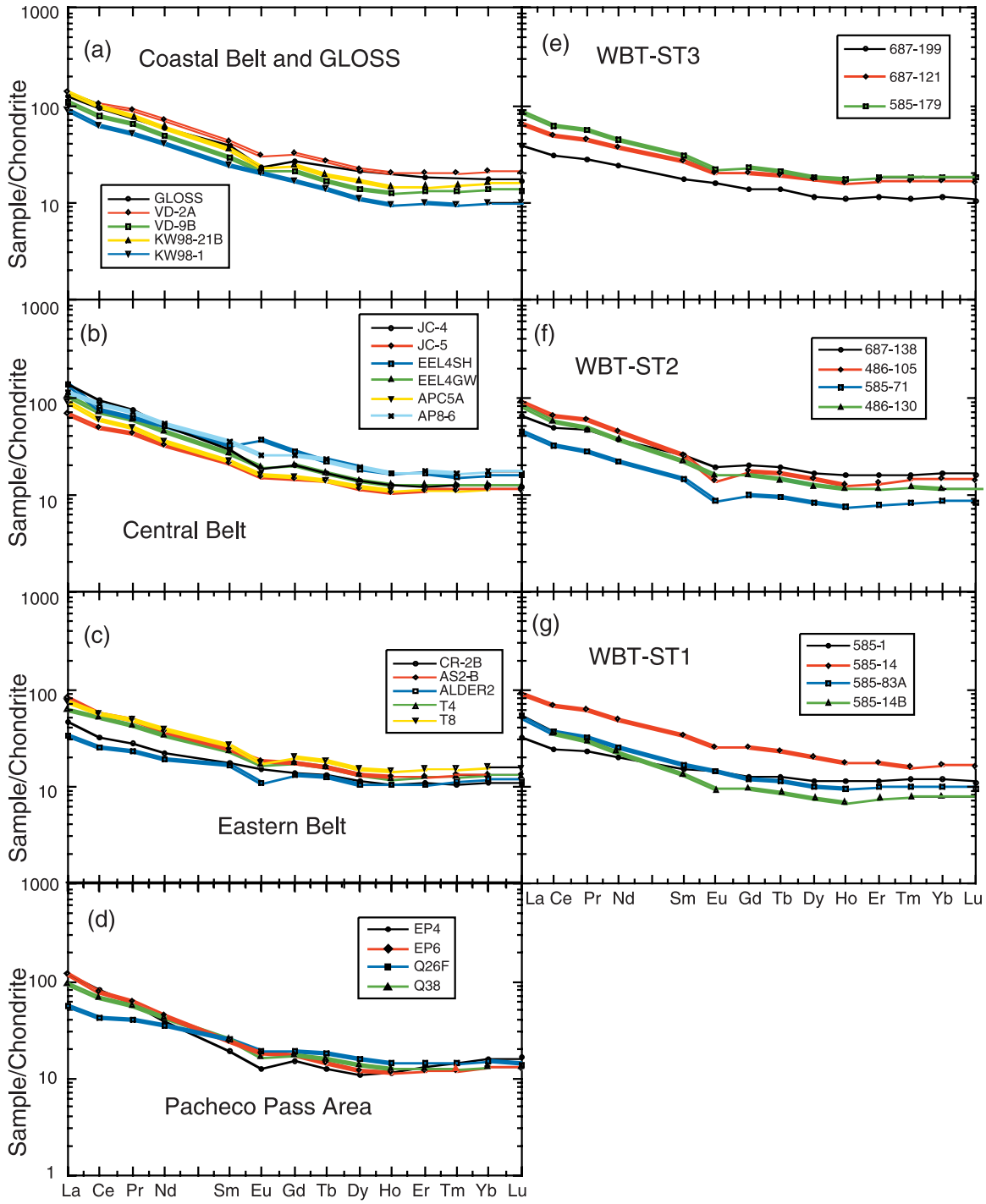

Figure 7. Chondrite normalized rare earth element diagrams for the various subunits of the Franciscan and WBT analyzed in this study. The composition of average subducting sediment (GLOSS [*Plank and Langmuir*, 1998]) is shown (a) with the lowest-grade rocks of the Coastal Belt, and it is apparent that these rocks are representative of common subducting sediments. Similarly, these REE values correspond to values for continental arc turbidites [*McLennan*, 1990]. (c, f, g) Some of the higher-grade units show slightly lower values for the light rare earth elements.

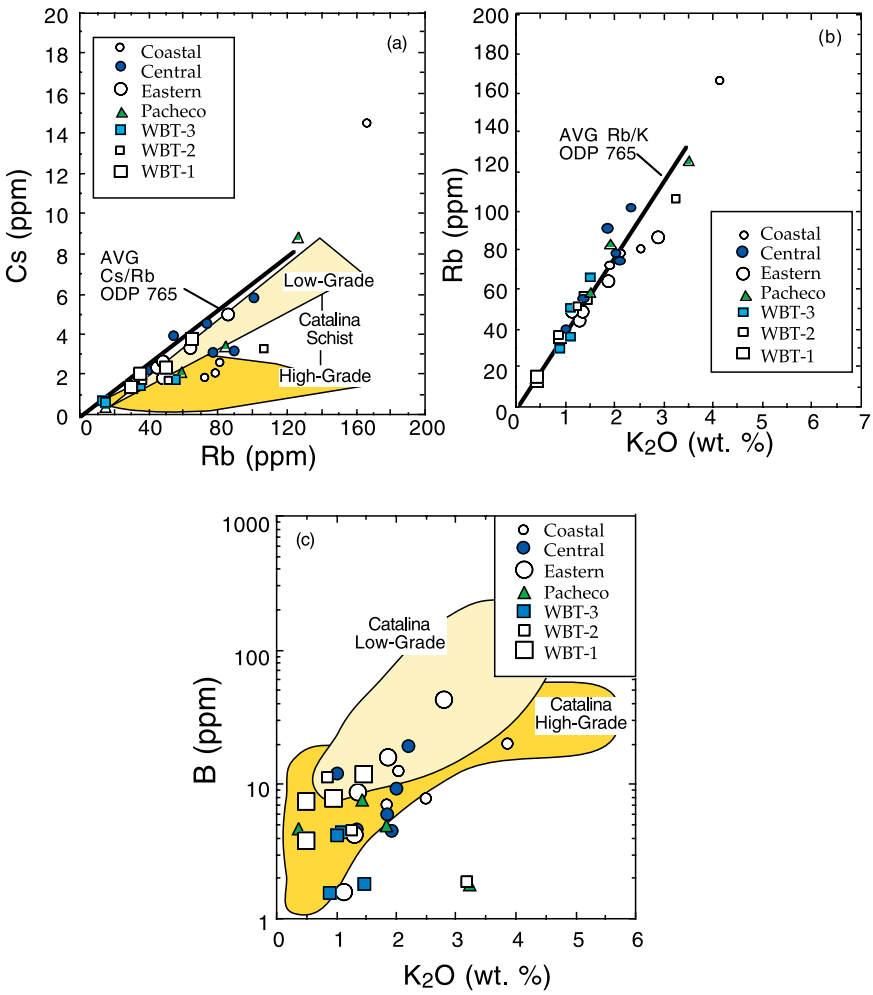

Figure 8. Most of the samples from this study show strong correlation of the various alkali elements, in contrast to the Catalina Schist, which shows progressive depletions in Cs and B with increasing grade [see *Bebout et al.*, 1999].

(see line on Figure 10a). In the Central Belt, N content ranges from 108 to 600 ppm with a very narrow range in $\delta^{15}N$ (+1.2 to +1.7‰; field on Figure 10a). Eastern Belt metasedimentary rocks have similar N concentrations (142 to 777 ppm) and range in $\delta^{15}N$ from +1.0 to +1.8‰, with one mafic sample containing 30 ppm N with $\delta^{15}N$ = +0.3‰. Samples from the Pacheco Pass area and the Western Baja Terrane contain amounts of N similar to those for samples from the Coast Ranges (Pacheco: 58–801 ppm, WBT: 121–692 ppm), with ranges in $\delta^{15}N$ that span the entire Coast Ranges data set (Pacheco: +0.2 to +2.2‰ and WBT: +0.1 to +2.8‰). C/N ratios of the various suites range from 1 to 60, with the lowest-grade Coastal Belt metasedimentary rocks showing the most uniform ratios similar to those of seafloor sediments (shaded field on Figure 10b).

5. Discussion

5.1. Lithological Representation of Subducting Sediments

[16] Samples of metamorphosed clastic rocks from the Franciscan Complex and Western Baja Terrane have major-element compositions that are, in gen-

Notes to Table 4
[a] Three replicates:, ppm = 738, 734, and 772; $\delta^{15}N$ = 2.7, 3.0, and 2.8.
[b] Internal N standard, 1σ = 259, and 0.14 respectively; n = 7. See *Sadofsky and Bebout* [2000] for more analytical details.
[c] Graphite standard for C-Isotope analysis of reduced C, 1s = 0.14 ‰, n = 8. Accepted $\delta^{13}C_{VPDB}$ value is −16.0 ‰.
[d] Internal carbonate standard, 1σ = 0.07 for $\delta^{13}C$ and 0.06 for $\delta^{18}O$, n = 8.

Table 4. C- and N-Concentrations and Isotope Compositions of Franciscan and WBT Samples

		Nitrogen		C-Reduced		Calcite Cement				
Site	Sample	ppm	$\delta^{15}N_{air}$	Wt. %	$\delta^{13}C_{VPDB}$	C/N	$\delta^{13}C_{VPDB}$	$\delta^{18}O_{VSMOW}$	Wt. %	$\Delta^{13}C_{ox\text{-}red}$
Coast Ranges-Coastal										
97-1	VD 2a	891	3.0	0.89	−25.2	10	-	-	-	
97-1	VD 5c	503	2.4	0.56	−25.3	11.2	−4.0	14.9	0.67	21.3
97-1	VD 9b	256	2.4	0.32	−25.3	12.4	−11.2	16.3	4.72	14.1
97-2	Mendo 8	748[a]	2.8[a]	0.79	−25.4	10.6	-	-	-	
97-2	Mendo 4	-	-	0.57	−25.4	-	−7.0	16.6	0.05	18.4
98-1	KW98-14a	689	3.4	0.61	−24.9	8.8	-	-	-	
98-1	KW98-21a	102	-	0.11	−25.1	10.4	-	-	-	
98-1	KW98-21b	106	1.4	0.16	−25.2	14.9	-	-	-	
98-1	KW98-1	-	-	0.16	−25.4	-	−5.0	17.5	11.7	20.4
98-1	KW98-52	-	-	0.13	−25.0	-	−4.1	17.4	6.41	20.9
98-3	KW98-91	209	-	0.27	−24.5	13.1	−5.5	17.2	12	19.0
98-3	KW98-93	677	2.9	0.61	−25.8	9.1	−0.4	13.7	3.76	25.4
Coast Ranges-Central										
97-3	Eel4 Shale	380	1.5	0.9	−24.2	23.7	−8.6	15.5	0.27	15.7
97-3	Eel4 GW	137	-	0.13	−25.0	9.8	−13.4	12.8	0.12	11.6
97-4	JC c4a	675	1.3	1.15	−24.7	17.1	-	-	-	
97-4	JC 5	214	1.5	1.24	−24.6	57.8	-	-	0.11	
97-4	JC 6	599	1.7	0.13	−25.0	2.2	-	-	-	
98-4	P&S 2a	-	-	0.03	−25.1	-	−2.9	14.2	7.42	22.2
97-5	AP c5b	108	1.7	0.38	−24.8	35.3	-	-	-	
97-5	APc5a	219	1.6	0.08	−28.2	3.4	-	-	-	
97-5	AP 8	195	1.2	0.17	−25.6	8.5	−10.1	12.8	1.68	15.5
Coast Ranges-Eastern										
97-6	CR 2b	777	1.0	0.09	−23.8	1.2				
97-6	CR1a2 mafic	30	0.3	0.02	−25.9	6.7				
97-7	Alder 1c	604	1.4	1	−25.7	16.5				
97-7	Alder 2	385	1.8	0.35	−26.7	9				
97-7	Alder 4b2	-	-	0.3	−26.7	-				
98-5	AS2-b	142	-	0.13	−27.2	9.3				
Pacheco Pass Area										
	WGE-Q34	166	2.2	0.2	−24.5	12				
	WGE-Q26f	36	0.7	0.04	−26.0	11.7				
	WGE-Q20	170	1.5	0.08	−24.7	4.4				
	WGE-Q38	166	2.1	0.23	−24.2	13.7				
	WGE-Q26g	58	1.1	0.05	−26.8	8.7				
	6-4-8-1	801	0.6	-	-	-				
	6-4-1-1	463	0.2	-	-	-				
San Simeon										
	SS3-1	866	2.2	-	-	-				
	SS2-1	559	1.9	-	-	-				
Cedros Island Sites-see *Sedlock* [1988]										
Western Baja Terrane-ST1										
	RLS-585-1	226	1.9	0.21	−28.8	9.3				
	RLS-585-14	305	0.1	0.19	−25.3	-				
	RLS-585-83a	-	-	0.06	−23.4	-				
Western Baja Terrane-ST2										
	RLS-486-105	692	2.5	0.1	−25.5	1.4				
	RLS-585-71	425	1.9	0.37	−24.2	8.7				
Western Baja Terrane-ST3										
	RLS-486-130	300	2.8	0.09	−23.3	2.9				
	RLS-585-133	121	-	0.24	−21.9	19.6				
	RLS-585-121	-	-	0.06	−25.1	-				
	RLS-585-179	-	-	0.11	−25.1	-				
	RLS-687-93	201	-	0.18	−22.3	8.9				
	T54[b]	4183	0.6							
	USGS 24				−16.4[c]					
	8-3-7v						−4.37[d]	14.74[d]		

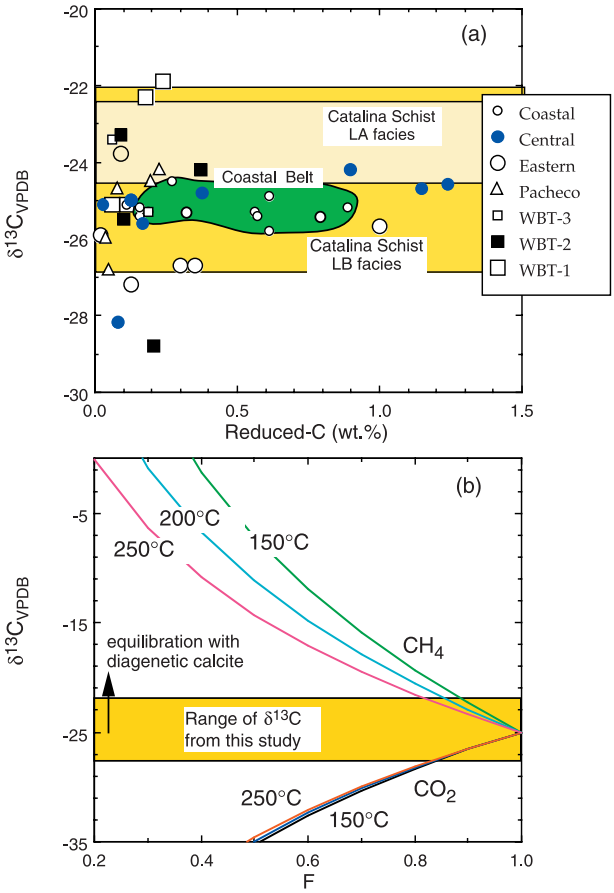

Figure 9. (a) Concentration and $\delta^{13}C_{VPDB}$ of the reduced (i.e., not carbonate) carbon present in these rocks. Most modern organic sediments have $\delta^{13}C_{VPDB} \sim -25‰$, although there are significant variations in these values due to various surficial and diagenetic processes [e.g., *Fogel and Cifuentes*, 1993]. Shaded fields represent $\delta^{13}C$ of metasedimentary rocks from the Catalina Schist lawsonite-albite and lawsonite-blueschist facies units. (b) Simple Rayleigh distillation models for the evolution of the host-rock $\delta^{13}C$ due to devolatilization of organic matter by a CH_4- or CO_2-rich fluid at a variety of temperatures.

eral, similar to those of sandstone-shale mixtures from modern oceanic trenches. Figure 4 shows SiO_2 and Al_2O_3 contents of the rocks from this study (broken down by subterrane) and values of similar sedimentary rocks and other subduction-zone-metamorphosed suites. Al_2O_3 and SiO_2 are closely correlated in these rocks and the other reference materials shown on Figure 4. Extremes are represented by the high-Al, low-Si, fine-grained metasedimentary rocks of the Catalina Schist, and some high-Si rocks from the Japan Trench and Sambagawa Belt (containing a large component of hydrous biogenic silica). Departures from a linear array of SiO_2 versus Al_2O_3 are caused by rocks containing abundant non-silicate phases such as calcite, or apatite in the case of one sample for the Central Belt of the Coast Ranges evident on this diagram (with 9.06 wt.% P_2O_5 and 13.84 wt.% CaO).

[17] A comparison of the bulk geochemistry of the samples analyzed in this study with the geochem-

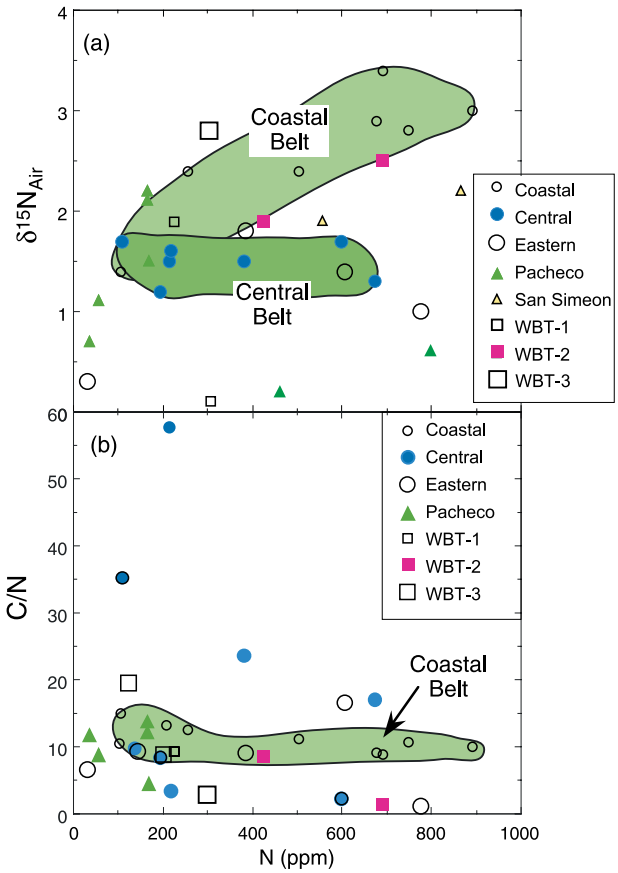

Figure 10. (a) Concentration and $\delta^{15}N_{air}$ of nitrogen in these rocks. Nitrogen content appears to vary mainly as a function of sedimentary protolith, and $\delta^{15}N$ values are similar to those expected in sediments with organic matter derived primarily from photosynthesizing organisms [see *Rau et al.*, 1987]. Metamorphic devolatilization of N (as N_2) would produce a trend of increasing $\delta^{15}N$ with decreasing N content as N-bearing fluid preferentially fractionates the lighter isotope. The ranges of compositions of the Coastal, Central, and Eastern Belts of the Coast Ranges are discussed in the text. (b) C/N versus N contents of the same rocks, demonstrating the lowest-grade Coastal Belt, Coast Ranges (patterned field), retains the most uniform C/N, independent of N concentration and thus appears to record the least devolatilization effect.

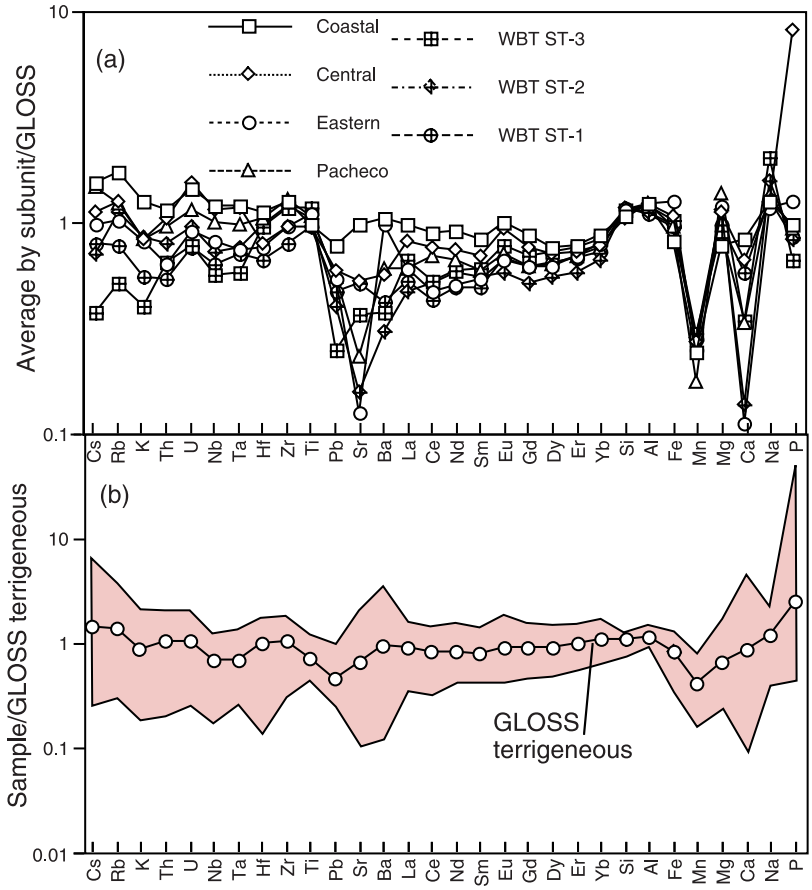

Figure 11. (a) Chemical compositions of the rocks analyzed in this study are averaged by lithotectonic subunit and normalized to the GLOSS estimate of average subducting sediments [*Plank and Langmuir*, 1998]. (b) Average value and range of compositions of samples from this study normalized to the average composition of ''terrigeneous'' sediments from the GLOSS database. Note that the scale of Figure 11a differs from that of Figure 11b.

istry of global subducting sediments shows that, for most elements, these rocks are representative of the geochemical composition of actively subducting clastic trench sediments. Individual rock compositions vary significantly, but the average compositions of each subunit are, in general, very similar to the average composition of subducting sediments (GLOSS [*Plank and Langmuir*, 1998]), in their concentrations of the large ion lithophile elements, high field strength elements, rare earth elements, and many of the major elements (Figure 11a). Significant departures from the GLOSS composition occur for Ca and Sr, which are depleted in many of the higher-grade samples of this study, likely partly because of the mobilization of calcium carbonate during devolatilization reactions. Part of this difference, however, is due to the inclusion of some pelagic carbonate (rich in CaO and Sr) in the GLOSS global composite. Manganese is depleted, relative to GLOSS, in most of these samples, because the Mn content of GLOSS is highly dependent on the abundance of hydrothermally produced clays and pelagic clays that are not abundant in these samples. More subtle suggestions of variations among different subunits of this study and between these rocks and GLOSS, such as variations in Pb, Ba, LREE, and LILE concentrations (Figure 11a), will be explained later in the discussion section.

[18] Comparison of the compositions of the samples from this study with the terrigeneous portion of subducting sediments (~76 volume % of the GLOSS global composite), derived by a simple average of the terrigeneous sediments from the

GLOSS database of *Plank and Langmuir* [1998] (Figure 11b), shows that the rocks from this study are very similar to the terrigeneous sediments present outboard of several active subduction zones. In fact, aside from the elements that are most variable in concentration in the rocks from this study, concentrations of most elements are virtually indistinguishable from the concentrations seen in the GLOSS estimate of terrigeneous sediments (for elements included in the GLOSS database).

[19] Potassium content also varies primarily with clastic lithology (Figure 5a) with higher K_2O contents in the shalier (lower SiO_2/Al_2O_3) rocks. Most of these rocks contain similar, or slightly lower, quantities of K_2O, relative to Al_2O_3, as sediments outboard of active subduction zones. This suggests that these rocks represent a reasonable range of bulk compositions and sandstone-shale proportions. The rocks analyzed in this study tend not to be as rich in K_2O as some of the metasedimentary samples of the Catalina Schist. Note also that some of the seafloor sediments (Japan Trench, Nankai) show a range to much higher SiO_2/Al_2O_3 than those of this study and the other suites presented for comparison: this is likely due to the dilution of the greywacke signal by siliceous oozes in these suites. Sodium is less systematic than K_2O in its variation with the other sandstone/shale indicators (Figure 5b). Despite the greater scatter in Na_2O vs. SiO_2/Al_2O_3, the same trend as seen in the K_2O data is apparent, with most samples showing Na_2O concentration similar to that of other likely subducted sediments. It is not surprising the K_2O and Na_2O concentrations are somewhat variable, given the possible exchange of these elements both between minerals during albitization of feldspars [see *Boles and Ramseyer*, 1988; *Morad*, 1988], illitization of clays and growth of white micas, and potentially, related to mobilization of these elements in diagenetic fluids.

[20] Rare earth elements from the Coastal and Central Belts of the Coast Ranges show chondrite-normalized patterns that are extremely similar to those of average continental arc turbidites [*McLennan*, 1990; *McLennan et al.*, 1990], clastic sediments of the Nankai Trough [*Pickering et al.*, 1993], and estimates for the global average of subducted sediment [*Plank and Langmuir*, 1998] (see Figures 7a and 7b; chondrite normalization values from *McDonough and Sun* [1995]). A few samples from the other subunits, particularly the Eastern Belt of the Coast Ranges and subterrane 1 of the WBT (Figures 7c, 7f, and 7g), appear be somewhat more depleted in the LREE (La-Sm) compared to those of the Coastal and Central Belts of the Franciscan. Mobilization of the LREE during low-grade subduction-zone metamorphism has been hypothesized because of the results of hydrothermal experiments showing that these elements can be mobilized into a fluid phase at low-T [*You et al.*, 1996]. However, the irregularity of the deviations from likely protolith values suggests that the deviations seen here are probably due to heterogeneity of the sediments rather than mobilization of the LREE. Relative REE enrichment can also be understood by examining ratios of light and heavy REE in order to determine if the differences observed above are significant. La/Sm is a measure of the degree of LREE enrichment and should be very high if the sediments are derived from continental sources and lower if the sediments are derived from arc volcanics. Yb/Sm should show the opposite trend. A plot of La/Sm vs. Yb/Sm (Figure 12) shows some of the types of possible provenance-related variation that are present in these rocks.

[21] Based on the La-Sm-Yb relationships (see Figure 12), samples from the Coastal and Central belts of the Franciscan appear to be derived from more "continental" sources, whereas some of the samples of the WBT and the Eastern Belt of the Franciscan show a trend toward arc-volcanic sources. This is not the first study to observe a difference in provenance between the Coastal Belt and the older units of the Coast Ranges; zircon fission track results [*Tagami and Dumitru*, 1996] suggest that the Coastal Belt contains a source younger than most of the Sierra Nevada, and sandstone petrofacies interpretations [*Underwood and Bachman*, 1986] suggest that this component may be derived from the Idaho Batholith.

[22] High field strength elements such as Ti, Nb, and Zr are present in concentrations similar to those of the expected protoliths (Figure 13). Tita-

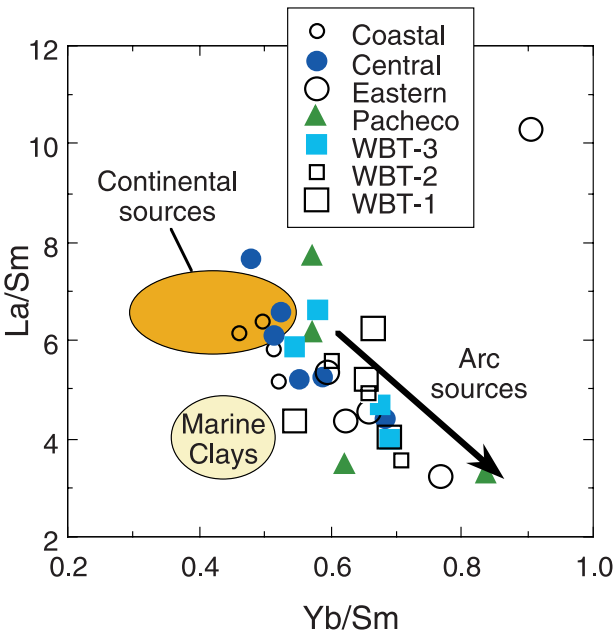

Figure 12. Paired examination of La/Sm and Yb/Sm ratios show the true slopes of the Rare Earth Elements. Samples from this study show that these sediments are derived primarily from "continental" and arc sources with some minor input from marine clays. Variations in provenance among the different subunits are somewhat ambiguous on this diagram, but it appears that the Coastal Belt represents more continental-derived material and the Eastern Belt contains more arc-volcanic material. Field of continental sources includes NASC, PAAS and estimated upper crust [*Taylor and McLennan*, 1985], and other continentally derived sediments of *Plank and Langmuir* [1998]. Fields for arc volcanic sediments and marine clays are from *Plank and Langmuir* [1998]. The one sample that with unusually high La and Yb relative to Sm is probably derived from sediments related to hydrothermal alteration [i.e., *Barrett and Jarvis*, 1988].

nium clearly co-varies with Al_2O_3 concentration, suggesting that it is enriched in the more clay-rich layers. Niobium and Zr concentrations vary significantly, but the values are well within the range of those summarized for subducting sediments [*Plank and Langmuir*, 1998]. Uranium is closely correlated with Zr in concentration (Figure 14a), suggesting that some of the U is present in Zr minerals. Lead is also correlated in concentration with Zr, although there is more variability in the correlation suggesting that some Pb may be present in other phases, such as sulfides (Figure 14b). Uranium/thorium ratios are nearly constant in these rocks, ranging from 0.22 to 0.41 (mean = 0.33 identical to the average U/Th of subducting terrige-

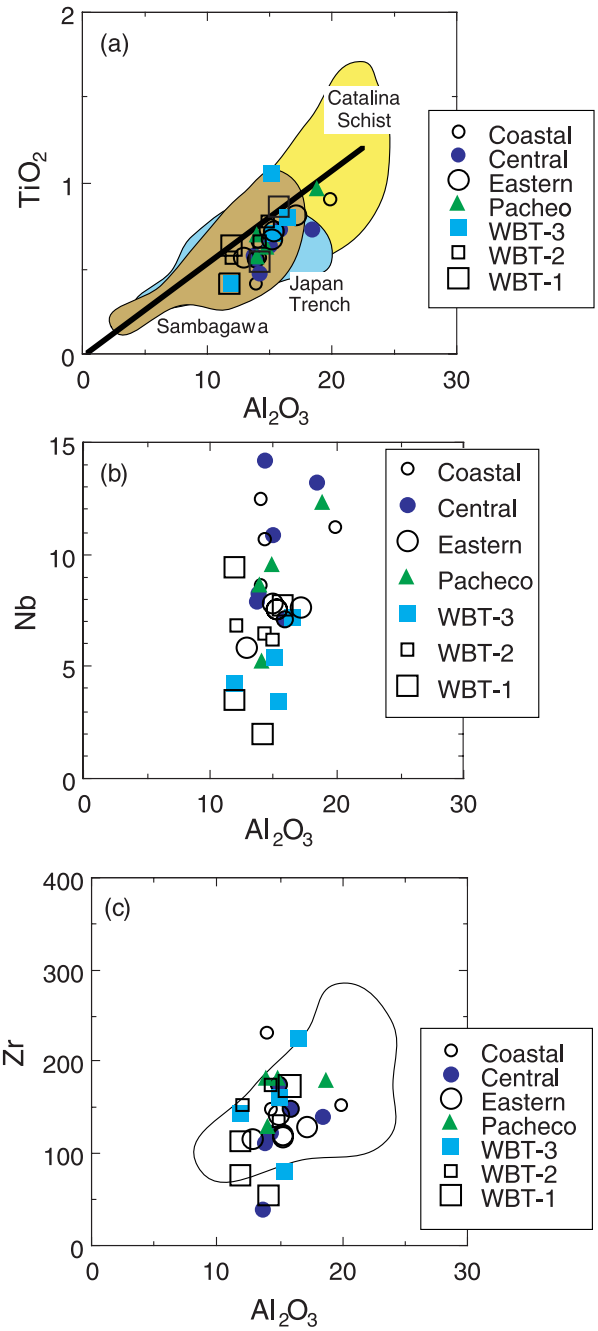

Figure 13. Variations of the High Field Strength Elements in rocks from the Franciscan and WBT. (a) TiO_2 (wt. %) varies nearly linearly with Al_2O_3 (wt. %) in rocks from this study and other analogues and protoliths; the thick line in Figure 13a shows a linear regression of turbidites from ODP site 765. (b) Nb (ppm) shows little correlation with Al_2O_3, with higher concentrations in the Coastal and Central Belts of the Franciscan and lower concentrations in the WBT. This Nb variation may suggest a difference in provenance between the Coast Ranges and the WBT. (c) Zr (ppm) concentrations are closely tied to Al_2O_3 and do not appear to vary significantly among the different sub-units.

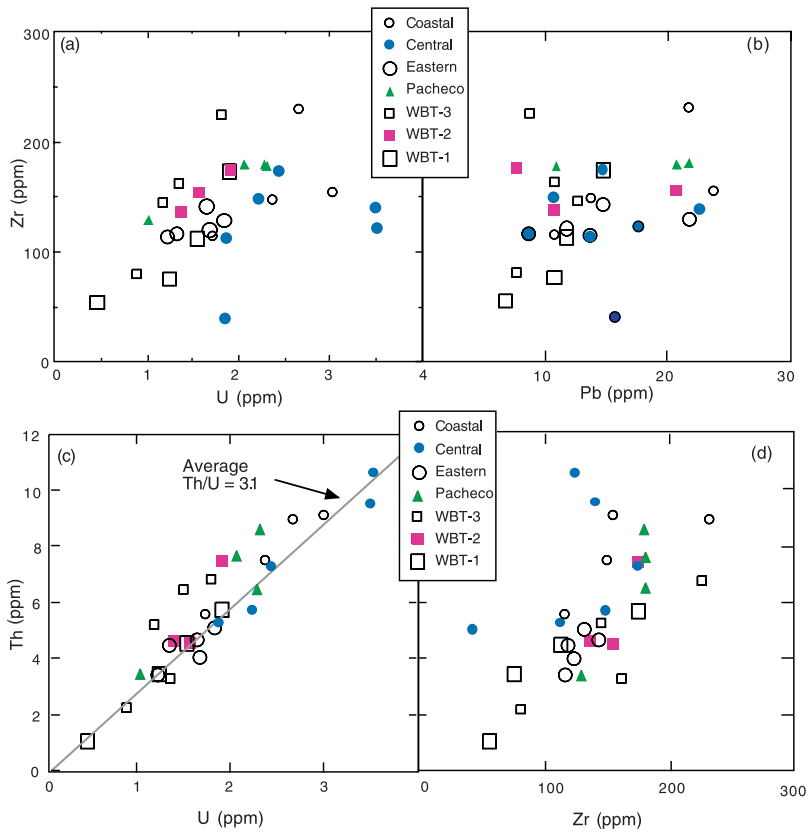

Figure 14. Uranium, thorium and lead variations in the Franciscan and WBT. (a) Uranium appears to vary nearly linearly with Zr content, suggesting the most U is bound in Zr phases. (b) Lead is more variable as a function of Zr than U, suggesting that there may be some Pb present in other phases such as sulfides. (c) Th/U ratios are nearly constant and Th/Zr is similar in variability to U/Zr (d), suggesting that Th and U are sequestered into these rocks by the same processes.

neous sediments in the GLOSS database [*Plank and Langmuir*, 1998]). The U/Th ratios from this study are also very similar to the lower-grade units of the Catalina Schist [see *Bebout et al.*, 1999]. The relatively constant ratios of U/Th and U and Th to Zr, suggest that the U and Th are usually present in the same detrital phases (see Figures 14c and 14d), or that Zr minerals and other actinide carriers (such as apatite and titanite with appropriate U/Th) are generally present in similar proportions in these rocks. The few outliers of high U/Zr and Th/Zr are most likely due to the addition of a surplus of other actinide carriers.

5.2. Evidence for Devolatilization and Effects on Rock Composition

[23] The Franciscan Complex and WBT contain rocks that have experienced metamorphic conditions varying from only very mild, incipient metamorphism to blueschist-facies conditions of up to 1 GPa and 300°C. Significant differences in mineralogy in these suites (for the Franciscan Complex, see Table 1) afford some reconstruction of their recrystallization histories and consideration of differential devolatilization in the units.

[24] The sedimentary protoliths of the Franciscan Complex and WBT rocks were composed of a mix of coarse-grained clastic detrital grains, detrital and pelagic clays, and pelagic silica ooze. Most of the samples selected for this study are greywackes primarily composed of clastic detritus deposited as variably bedded turbidites. The non-clay fraction of detrital grains present in these rocks appears mainly to have been a mix of quartz, feldspars, lithic clasts (volcanic and sedimentary), and a significant component of less-stable minerals such as micas (see Table 1) [*Underwood and Bachman*, 1986; *Sedlock*, 1988]. Sedimentary clay mineral

composition is more difficult to determine, as the clays are both finer-grained and more reactive than the other clasts. However, clay-mineral analysis of other accretionary wedge and trench sediments suggests that these rocks probably contained a variety of sedimentary clay minerals such as chlorite, illite, smectite, kaolinite and montmorilinite, and some mixed-layer clays [i.e., *Karnosov et al.*, 1977; *Karpoff*, 1992; *Underwood and Deng*, 1997] (ODP-Leg 185). Clay minerals have variable, but high, water contents; ideal kaolinite ($Al_2Si_2O_5$ $(OH)_4$) contains 14 wt.% H_2O and most illites contain ~10 wt.% H_2O (for comparison, white-micas, stabilized at higher grades by the breakdown of clays, contain ~5 wt.% H_2O).

[25] As these sediments progressed downward in the subduction zone, they underwent mineralogical changes that must have resulted in significant chemical redistribution, at least at the local scale. Even the lowest-grade rocks of the Coastal Belt differ from likely sedimentary protoliths in several important ways. There is a loss of porosity associated with initial subduction, which may be closely related to the production of abundant veins containing quartz, calcite, laumontite or a combination of these minerals. Many obviously detrital grains remain in these rocks, but there appears to be significant sericitization of feldspars; detrital clays and micas are likely to have transformed to more crystalline clays and fine-grained, celadonitic white micas; and organic matter has somewhat matured as indicated by vitrinite reflectance [*Underwood and Bachman*, 1986].

[26] In the higher-grade sub-units, many more changes took place and likely participated in the redistribution of volatiles and trace elements. Carbonaceous matter became increasingly crystalline, and vitrinite reflectance, along with mineral assemblage, serves as the basis for many of the estimates of peak-T conditions throughout the Franciscan Complex and WBT [see *Bostick*, 1974; *Larue*, 1986; *Blake et al.*, 1987; *Sedlock*, 1988]. This maturation of organic matter corresponds to increasing chemical purity (i.e., lowered concentrations of H, N, and S [see *Teichmüller*, 1987]), and therefore, liberation of the non-C components of sedimentary organic matter. Detrital K-feldspar was replaced by albite, thereby liberating K^+ that may be incorporated into micas or mobilized into metamorphic fluids, and requiring a source of Na^+ [see *Morad*, 1988]. The large amount of variation in Na^+/K^+ among samples of single units, together with significant overlap in this ratio for the various units, prevents the identification of any whole-rock effect of open-system Na^+-K^+ exchange. Detrital weathered micas, chlorite, and clays were transformed into more crystalline clays, stilpnomelane, and white micas [i.e., *Dalla Torre et al.*, 1996], and this transformation was likely accompanied by a release of H_2O. This breakdown of clay minerals may also have mobilized trace elements such as Rb, Cs, and B that are concentrated in detrital clays [see *Moran et al.*, 1992; *Plank and Langmuir*, 1998]. Lawsonite is present in most samples from everywhere except the Coastal Belt and is likely to have formed from dehydration reactions that consume laumontite or other zeolite minerals, or from decarbonation reactions involving carbonate cements.

[27] Loss on ignition (i.e., total volatile content, in most cases, mainly H_2O) appears to vary primarily as a function of sedimentary lithology in the rocks from this study, and there does not appear to be systematic variation as a function of metamorphic grade (Figure 6). However, the rocks from this study, as well as other low-grade subduction-zone metamorphic rocks from the Catalina Schist and the Sambagawa Belt, appear as a whole to be significantly lower in total structurally-bound volatile content than many similar lithologies collected on the ocean floor and deep in sediment cores. In contrast, higher-grade rocks of the Catalina Schist show significant variations in LOI as a function of grade, even at high Al contents (see Figure 6). That samples from these suites are lower in total volatile content than sediments collected from the ocean floor, and that there is no significant variation in LOI of these rocks as a function of relative grade (when normalized for SiO_2/Al_2O_3), suggests that there has been some significant loss of water or other volatile components during the earliest stages of lithification and diagenesis of these rocks in the subduction zone (i.e., at depths of <10 km). The logical reactions that

would be expected to cause this decrease in total LOI even in the lowest-grade rocks would be clay mineral transformations and mica growth (i.e., smectite/illite transition) and dewatering of any opal (~4–9 wt.% H_2O) that was present. This significant difference in LOI between modern sediments and the lowest-grade metamorphic rocks of the Franciscan Complex suggests that some caution must be exercised in the use of modern seafloor sediments to estimate the quantity of structurally bound H_2O that is deeply subducted [cf. *Bebout*, 1996]. Note that these discussions consider only the structurally bound volatile component in subducting marine sediments and do not consider the large amount of pore fluid thought to be mechanically expelled at shallow levels [cf. *von Huene and Scholl*, 1991].

[28] Rocks from the Franciscan Complex contain relatively abundant reduced C (up to ~1.3 wt.%), with most samples having $\delta^{13}C$ values of ~−25‰ (almost all $\delta^{13}C$ are −25‰ ± 1.5‰). This $\delta^{13}C$ is very similar to average marine organic matter [i.e., *Deines*, 1980]. The relatively narrow range in $\delta^{13}C$ of the Coast Ranges samples (Figure 9a) suggests that most of these rocks have not experienced significant devolatilization of carbonaceous-C, as low-T loss of C as CH_4 or CO_2 in fluids would create a significant shift in $\delta^{13}C$ (see the calculations in Figure 9b). Some of the other samples from the Pacheco Pass area and the higher-grade rocks of the Western Baja Terrane (and one sample from the Central Belt) do show shifts in $\delta^{13}C$ (Figure 9a). This C-isotope data set is comparable with the C-isotope data set for the low-grade units of the Catalina Schist, in which lawsonite-albite facies rocks show extremely uniform $\delta^{13}C$ and lawsonite-blueschist facies rocks show somewhat greater variability and are somewhat shifted isotopically to heavier values [see *Bebout*, 1995] (ranges on Figure 9a). There are two likely causes of this variability in $\delta^{13}C$ of reduced-C; devolatilization-related shifts in $\delta^{13}C$ (Figure 9b), and partial metamorphic equilibration of the reduced-C with diagenetic $CaCO_3$. The calcite cement retained in samples from the lower-grade rocks varies in isotopic composition even at a single outcrop (with constant reduced C-$\delta^{13}C$; see Table 4), suggesting that the cement and reduced C have not fully equilibrated with respect to C-isotopic composition (see the highly variable $\Delta^{13}C_{calcite\text{-}cm}$ in Table 4). However, the lack of full equilibration of C-isotopes in the lower-grade rocks does not rule out partial exchange of C among reduced and oxidized C reservoirs, especially at higher grades/temperatures. That several samples show increases in $\delta^{13}C$ and a few samples appear to show decreases in $\delta^{13}C$ is somewhat problematic in attempting to point to an individual metamorphic pathway for the shifts in $\delta^{13}C$. However, it is possible to produce shifts to higher $\delta^{13}C$ of the reduced-C due to devolatilization of a CH_4-rich fluid or by interaction with marine carbonates, or to lower $\delta^{13}C$ by devolatilization of a CO_2-rich fluid (see Figure 9b; fractionation data from *Richet et al.* [1977]). Additionally, the few samples with somewhat higher $\delta^{13}C$ are relatively low in organic-C content and may originally have had significant carbonate cement. Sandstones would be likely to have a high ratio of carbonate to organic C, whereas shalier lithologies would be likely to contain more carbonaceous matter and smaller amounts of carbonate cement. If this carbonate cement was lost to metamorphic reactions and was able to react (even slightly) with the reduced-C reservoir in the rock, then it could produce a shift in the $\delta^{13}C$ of the remaining C. This potential shift in $\delta^{13}C$ would increase the $\delta^{13}C$ of the remaining reduced-C, and the magnitude of the increase would depend on the total ratio of oxidized to reduced-C involved in the reaction and, therefore, the original bulk $\delta^{13}C$ of the rocks. It should be noted that, although the $\delta^{13}C$ values are somewhat shifted in some of the higher-grade rocks of the Franciscan and Western Baja Terrane units, these shifts are relatively small compared with those of up to ~10‰ in epidote-blueschist facies and higher-grade metasedimentary units in the Catalina Schist [see *Bebout*, 1995].

[29] Carbonate cements appear to behave very differently than the reduced C present in these rocks. Greywackes from the Coastal Belt contain up to ~11 wt.% calcite cement (mean = 5 wt.%), and Central Belt samples contain up to ~7 wt.% (mean = 2 wt.%), but there is no appreciable calcite

cement remaining in the higher-grade rocks studied (similar to the observations made for the Catalina Schist [*Bebout*, 1995]). The estimates of average calcite cement content may be somewhat high because only those samples containing obvious calcite were analyzed for cement concentration and isotopic composition. By assuming that no cement is present in the samples for which it was not measured, a reasonable assumption based on petrographic observations and tests with HCL, and including those samples in an average, it is possible to derive some minimum estimates of carbonate cement concentration of each lithotectonic subunit. It appears that the Coastal Belt samples contain an average of >2% and that Central Belt samples average ~1% calcite cement. This calcite is absent in the higher-grade rocks. Correlated enrichment in elevated CaO and Sr concentrations is prominent in the lower-grade rocks (see data for the Coastal Belt in Figure 15), and the Central Belt (Coast Ranges) and ST-3 (the lowest-grade WBT unit) also have high Sr and/or CaO contents, possibly indicating that, for the higher-grade units, some Sr and Ca was mobilized in fluids during the decarbonation reactions that resulted in the removal of the diagenetic cement. These elements may then be consumed downstream by the creation of abundant Sr-rich, $CaCO_3$ veins (particularly if the veins are composed of aragonite, orthorhombic carbonate which more effectively sequesters Sr), or they may be the source of alkaline fluids such as those detected in the Marianas forearc (cf. *Fryer et al.* [1999] and discussion by *Sadofsky and Bebout* [2001a]).

[30] Nitrogen is bound into sediments both by sedimentation of N-bearing organic matter and by bonding of NH_4^+ and NO_3^- to clays, and it is therefore not surprising to see some variability in both N concentration and $\delta^{15}N$ in these rocks. Nitrogen derived from photosynthesizing organisms in sediments is usually close to 0‰ in $\delta^{15}N$, and NH_4^+ derived from higher organisms or NO_3^- adsorbed onto clay minerals is usually significantly higher in $\delta^{15}N$ (+7 to +11‰ [*Rau et al.*, 1987]). Most modern seafloor sediments have total-N $\delta^{15}N$ that is somewhat higher than that of the samples in this study [e.g., *Rau et al.*, 1987; *Macko*, 1989; *Muzuka et al.*, 1991]. A shift, with depth (0 to 220 m) in $\delta^{15}N$ in ODP Leg 185 sediments (Site 1149) from surface values near +8‰ to values at depth near +3‰, the latter similar to those for the high-P/T suites (Figure 10a), is consistent with diagenetic loss of a high-$\delta^{15}N$, perhaps NO_3^- component [*Sadofsky and Bebout*, 2001b]. All of the $\delta^{15}N$ values observed in the metasedimentary samples are closer to those expected for sedimentary N derived primarily from photosynthesizing organisms (Figure 10a). For all units but the Coastal Belt, Coast Ranges, there is no obvious correlation between N concentration and $\delta^{15}N$. Samples from the Coastal Belt show a trend toward higher $\delta^{15}N$ at higher N concentration, and the variations in $\delta^{15}N$ could be due to differential loss of heavy N as NO_3^- during diagenesis and extremely low-grade metamorphism accompanying subduction to these extremely shallow levels (<10 km [cf. *Sadofsky and Bebout*, 2001b]). Moving upgrade in the Coast Ranges, the more uniform $\delta^{15}N$ of the somewhat higher-grade (more deeply subducted; see Figure 3) Central Belt and Eastern Belt metasedimentary rocks could reflect the more

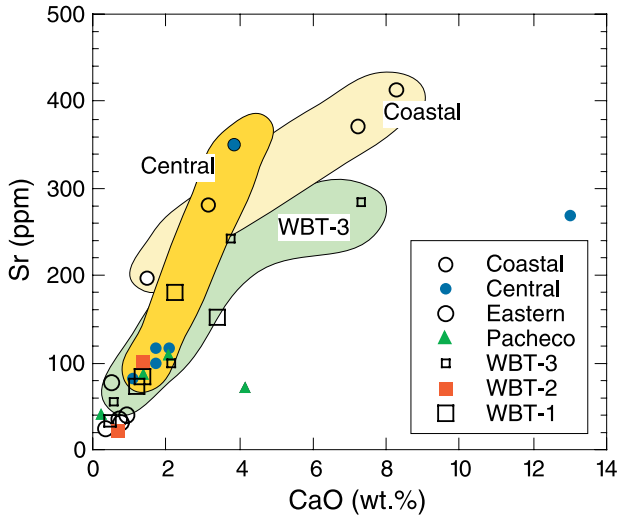

Figure 15. Sr and CaO variations in the Franciscan and WBT. Note that many of the lower-grade rocks of the Coastal and Central Belts (Coast Ranges) and the lowest-grade subunit of the WBT have CaO and Sr concentrations that are greatly enriched relative to most of the other samples. This Sr and Ca depletion may correspond to the mobilization of calcium carbonate during low-grade metamorphism of these rocks.

complete loss of this heavy NO_3^- (see data for the three Coast Ranges units in Figure 10a). Carbon-reduced/nitrogen ratios are another useful indicator of the devolatilization of these elements, as both of these elements are provided to the sedimentary rocks largely by organic processes. Most sediments should have C/N ratios <20:1 [*Müller*, 1977; *Sweeney et al.*, 1978; *Waples and Cunningham*, 1985], which would be likely to be fractionated if either element was being lost due to devolatilization as organic detritus becomes purified (ultimately to graphite) and N is transferred into phyllosilicates. The vast majority of the high-P/T metasedimentary rocks from this study fall into that range (Figure 10b). The Coastal Belt samples have C/N more uniform than that of the higher-grade units (Figure 10b), fully within the range for modern seafloor sediments, and perhaps indicating that the loss of isotopically heavy N as NO_3^- producing the decrease in whole-sediment $\delta^{15}N$ did not produce significant shifts in the C/N of the same sediments (i.e., the N adsorbed to clays was extremely heavy). The higher-grade Coast Ranges units show scatter in C/N and shifts mostly to higher C/N relative to C/N of the lowest-grade Central Belt, perhaps reflecting the effects of deeper metamorphic devolatilization (i.e., at depths of 10–40 km).

[31] Rubidium, Cs, and B were investigated in some detail because B and Cs show strong variations caused by differential devolatilization in the Catalina Schist [*Bebout et al.*, 1999] and because B, Cs, and Rb have been shown to devolatilize during low-T hydrothermal experiments [*You et al.*, 1996]. Sedimentary Rb and Cs concentrations vary mainly as a function of K as they substitute for K in potassic minerals. Figure 8 shows the variations in Rb, Cs, and B in the rocks from this study, and for reference, the Catalina Schist. Rubidium and Cs concentration are correlated with K_2O concentrations in these rocks, and the Rb/K_2O, Cs/Rb, and Cs/K_2O ratios are very similar to those of the turbidites from ODP site 765 [see *Plank and Langmuir*, 1998].

[32] Boron concentrations are generally somewhat lower than those observed in the low-grade units of the Catalina Schist, even at similar K_2O contents (Figure 8c). Boron, like N, is tied into sediments both as structurally bound B and as an adsorbed component and is commonly present in seafloor sediments at levels of up to ~300 ppm [see *Moran et al.*, 1992; *Ryan and Langmuir*, 1993; *Spivack et al.*, 1987; *Kopf and Deyhle*, 2002]. Boron, at concentrations of less than 50 ppm, is one of the only elements that is clearly depleted in these rocks relative to their protoliths. Because there does not appear to be any significant variation in the degree of depletion of B between the lower-grade and higher-grade rocks of this study, it appears that this depletion happened before reaching the conditions of the Coastal Belt. There is likely to be significantly more adsorbed B than structurally bound B present in the sedimentary protoliths of these rocks and loss of this adsorbed B to interstitial fluids during the early stages of diagenesis may provide the mechanism for B depletion from these rocks [see *Kopf et al.*, 2000]. Boron-isotopic study of the Catalina Schist demonstrated that the B present in the low-grade metasedimentary rocks of that suite is dominantly derived from the structurally bound B in sediments [*Bebout et al.*, 1998], and it is suggested that the B remaining in the rocks of this study is derived from sedimentary structurally bound B rather than previously adsorbed B being bound into clay minerals.

[33] Arsenic and Sb are also potentially useful indicators of devolatilization reactions, as they can be significantly fractionated out of a rock while many other less fluid-mobile elements remain [see *You et al.*, 1996; *Bebout et al.*, 1999]. However, As and Sb concentrations do not appear to vary in concentration as a function of grade in the Franciscan and Western Baja Terrane suites, and the As and Sb concentrations and As/Ce and Sb/Ce overlap strongly with those of the low-grade metasedimentary rocks in the Catalina Schist (Figures 16a and 16b). During metamorphism, As and Sb probably become coupled with S as they partition into sulfides [see *Noll et al.*, 1996; *Bebout et al.*, 1999]. However, there is very little correlation with S for either element in the rocks from this study (As/S ranges from 0.0005 to 0.15, Sb/S ranges from 0.00005 to 0.02). Sulfur concentration is highly variable in these rocks (see Table 3), ranging from the detection limits of XRF (50 ppm) to several

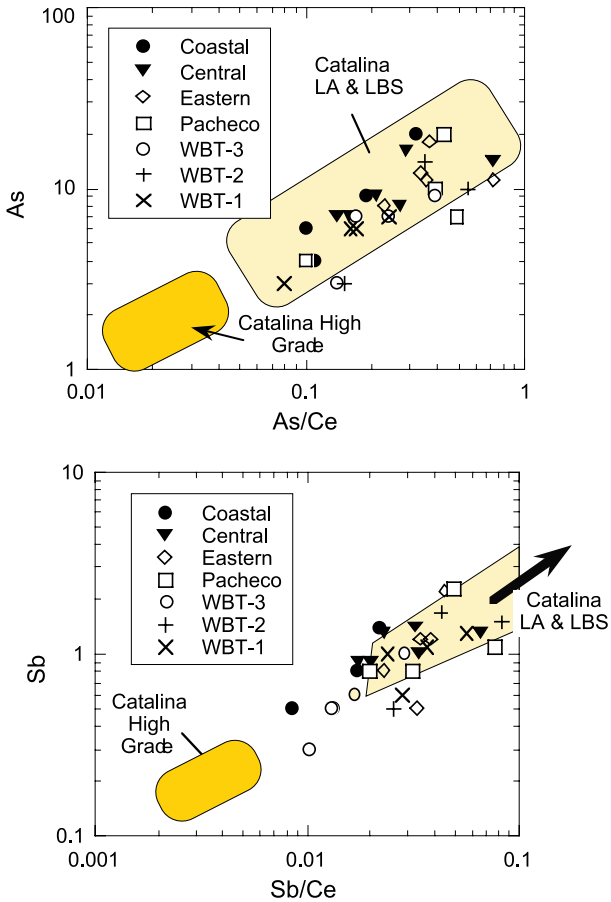

Figure 16. As (ppm) and Sb (ppm) are plotted against As/Ce and Sb/Ce because these parameters have been shown to vary significantly as a tracer of devolatilization of the siderophile elements [*Bebout et al.*, 1999]. These plots show that both As and Sb are similar in concentration to low-grade (LA and LBS facies) rocks of the Catalina Schist, and do not appear to be tracing more subtle variations in extents of metamorphic devolatilization among the lower-grade units.

thousand ppm, with variations of two orders of magnitude occurring even within single subunits. This variation in S content is likely due to protolith variations that could include both sulfides and sulfates (present in sediments and seawater [see *Alt and Burdett*, 1992]).

5.3. Comparison of the Results of This Study With Those of Hydrothermal Experiments

[34] One prior study has specifically attempted to determine the relative mobility of volatiles and fluid-mobile trace elements at low-T during subduction-zone metamorphism through hydrothermal experiments [*You et al.*, 1996]. Other studies have attempted to address element mobility during low-T hydrothermal experiments [i.e., *Seewald et al.*, 1990; *Sturtz*, 1991; *You et al.*, 1995]. These studies have been carried out at temperatures similar to the conditions experienced by the rocks from this study, but, due to experimental limitations, have been carried out at much lower pressures and high fluid: rock ratios (water/rock = 3 by weight [*You et al.*, 1996]). These studies have shown that As, Ba, B, Cs, NH_4+, Pb, Rb and the LREE are relatively mobile at T < 300°C, P < 0.1 GPa, and high fluid:rock ratios.

[35] Comparison of the data from this study with results from the hydrothermal experiments shows agreement in that the adsorbed components of B and N appear to be missing from the rocks of this study. However, the rocks studied here show retention of structurally bound As, Cs, Pb, Rb, the LREE, and structurally bound B and N, suggesting that the vast majority of the reservoirs of these elements are not mobilized at shallow depths during relatively low-T subduction zone metamorphism and are thus subducted to greater depths. The rocks analyzed as a part of this study do demonstrate significant protolith heterogeneity that may complicate the assessment of small degrees of element loss, and it is difficult to prove unequivocally that certain elements were not present in metamorphic fluids. However, the differences in apparent mobility of potentially fluid-mobile elements between this study and the results of hydrothermal experiments are more likely to be due to the strikingly different conditions encountered with far greater pressures in the natural system and at significantly lower fluid:rock ratios.

5.4. Implications for Models of Slab + Sediment to Arc Subduction Zone Mass Transfer

[36] Recent attempts to model the subduction input into the mantle [*Plank and Langmuir*, 1993, 1998] and the participation of sediments in arc magma generation [e.g., *Ryan et al.*, 1995, 1996; *Noll et al.*, 1996; *Elliott et al.*, 1997; *Patino et al.*, 2000], have either relied on elements not expected to

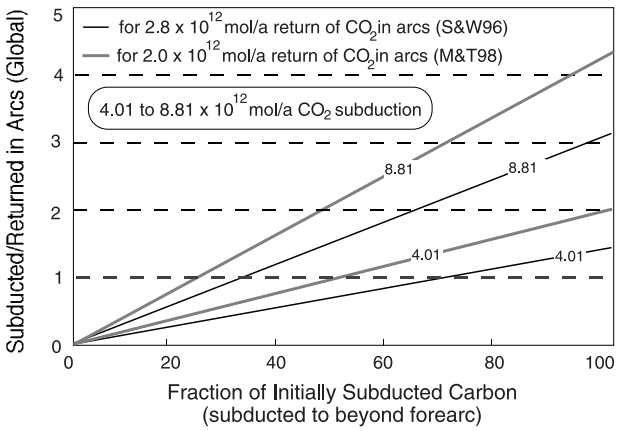

Figure 17. Example of an attempt to mass-balance subduction-zone inputs and outputs, in this case, for C (as both carbonate and reduced/organic C). The horizontal axis represents the efficiency with which C is returned via arc magmatism, and the multiple lines emanating from the origin represent the range of combinations of limits in estimates of the inputs and outputs (see text for discussion). A "subducted/returned" ratio of 1 indicates balance of the subducted C inventory with the C returned from the mantle in arcs.

mobilize during low-T metamorphism, assumed the effects of element mobility prior to the depth of arc magma generation were minimal, or been limited to only broad correlation of sediment source and arc output. This study demonstrates the retention of most of the trace elements regarded as relatively fluid-mobile (e.g., B, Cs, As, Sb) to depths of up to ~40 km during relatively cool subduction zone metamorphic conditions, and therefore helps to validate this approach for many elements—these elements would thus probably be available at greater depths to produce enrichments in arc lavas. Furthermore, the gradual loss during of these trace elements during devolatilization at depths of ~70–250 km could lead to across-arc trends in concentration and isotopic composition (see examples of cross-arc trace element variations in *Ryan et al.* [1995] and *Moriguti and Nakamura* [1998]). However, as examples, the observations regarding the significant loss of structurally bound H_2O, the mobility of adsorbed, likely isotopically distinct, B and N components, and the mobilization of Ca and Sr related to decarbonation, underscore the need to exercise caution in interpretations of arc-volcanic concentrations of these elements which directly employ the compositions of seafloor sediments as a mixing component.

5.5. Example of an Attempt to Balance Subduction Inputs and Outputs (C Subduction)

[37] Although uncertainties tend to be large, it is possible to estimate the fluxes of C into and out of the mantle and, in particular, the fluxes of C (and other volatiles) into and out of modern convergent margins (here done on a global basis; see the results of this calculation in Figure 17). Fluxes of C into subduction zones are based on (1) estimates of the volumes and lithology of sediment being subducted in modern subduction zones (e.g., based on the work of *von Huene and Scholl* [1991], *Rea and Ruff* [1996], *Plank and Langmuir* [1998]), (2) chemical and isotopic analyses of the sediments that are likely being subducted, and (3) for altered oceanic crust, estimates of carbonate content by *Staudigel et al.* [1989] [also see *Alt and Teagle*, 1999]. The estimates of carbon dioxide flux returned to the surface from arcs (on a global basis) are from *Marty and Tolstikhin* [1998] and *Sano and Williams* [1996]. For the calculations of subducted C flux presented here (range of 4.01 to 8.81 $\times$ 10^{12} moles/yr), we used the lithologic proportions of GLOSS (Global Subducting Sediment of *Plank and Langmuir* [1998]; 76 wt.% terrigeneous, 7 wt. % calcite), and a range of sediment subduction rates from *Plank and Langmuir* [1998] (1.3 $\times$ 10^{15} g/yr) and *von Huene and Scholl* [1991] (2.75 $\times$ 10^{15} g/yr). We attempt to consider only the part of the seafloor sediment column presently being deeply subducted, that is, to beyond the depths of accretion and underplating. The estimates of *von Huene and Scholl* [1991] attempt to take into account the underplated fraction (1.0 km^3, or 2.75 $\times$ 10^{15} g/yr of sediment) that is subducted to beyond depths of frontal and underplating accretionary processes, whereas the *Plank and Langmuir* [1998]; (1.3 $\times$ 10^{15} g/yr) estimate for modern sediment subduction accounts for only the incoming flux minus an estimate of the accretion flux (see recent discussion of sediment subduction and accretion by *Beaumont et al.* [1999]). We do not incorporate consideration

of subduction erosion (potentially extremely large, estimated by *von Huene and Scholl* [1991] to be 0.6 to 1.1 km^3/yr) into these illustrated flux calculations and, depending on the composition (and specifically the physical state and concentration of C) of the eroding hanging-wall, this could significantly impact the carbon dioxide flux estimates and estimates of the proportions of reduced and oxidized C in the subduction flux (see below). For C concentration in sediments we use an average of the results from this study and data from low-grade metasedimentary rocks of the Catalina Schist [*Bebout*, 1995]. For C flux in bulk oceanic crust, we use the estimates of *Staudigel et al.* [1989] (0.233 and 0.296 wt. % carbon dioxide calculated by two methods) and take into account a small range of estimates of oceanic crust subduction rates. Note that, for the various estimates of subduction C flux, the carbonate in the altered oceanic crust constitutes 45–65% of the C flux due to its greater subducted mass relative to the more C-rich sediments. Finally, we include a small amount of carbon dioxide in the terrigeneous sediment component as diagenetic cement (0.5 wt. %).

[38] Although it can perhaps be concluded with some certainty that more C is subducted than returned to the surface in arcs, the uncertainties in both the inputs and the outputs confound any truly quantitative assessment of return percentages. A roughly 40% (±20%) of the subducted C reservoir can balance the estimated return of C to the surface in arcs (Figure 17); if true, this would indicate that approximately 60% (±20%) of the subducted C is entrained into the deeper mantle, where it could contribute to mantle C budgets and perhaps contribute to C fluxes in ocean-island basalts and at mid-ocean ridges (see discussion by *Marty and Tolstikhin* [1998]). The conclusion that much of the C initially subducted is entrained into the deep mantle is consistent with the conclusion of *Kerrick and Connolly* [2001] that much of the subducted C inventory (particularly carbonate in the more pure limestone lithologies) is deeply subducted rather than released at shallower levels, based on calculated devolatilization histories for appropriate sedimentary lithologies. For many other volatiles and trace elements, such calculations are even more problematic because of the uncertainties in the compositions of subducting materials (e.g., for N, the concentrations and isotopic compositions in altered oceanic crust are unknown, and are likely to be quite heterogeneous). These comparisons underscore the utility of recent attempts to mass-balance materials across individual, relatively well-understood convergent margins where better-constrained inventories of subducting crust and sediment and arc magmatism can be incorporated.

6. Conclusions

[39] The Franciscan Complex and the Western Baja Terrane record retention of significant volatile contents (elements such as H, C, N, S) and fluid-mobile trace elements (B, Rb, Cs, As, Sb) in metasedimentary rocks to depths of up to ~40 km. Loss on ignition of these rocks appears to be lower than would be expected for modern sediments of similar clastic lithologies, suggesting that there was some loss of structurally bound H_2O during earlier diagenesis. However, there does not appear to be a trend of differential LOI as a function of metamorphic grade in these rocks, perhaps because these losses occurred primarily at shallower levels and lower temperatures than those experienced by all of the high-P/T metasedimentary suites. The LOI of the Franciscan Complex and the Western Baja Terrane metasedimentary rocks may be a good estimate for the volatile content retained to the next series of metamorphic transformations (overall, constituting the blueschist-to-eclogite facies). Nitrogen and B are both present at concentration levels that are consistent with the expected concentrations of the structurally bound components of these elements in the protoliths. Boron isotope data for lithologically and petrologically similar low-grade metasedimentary rocks in the Catalina Schist, California, are consistent with the shallow loss of isotopically heavy adsorbed B [*Bebout et al.*, 1998].

[40] Together, the reduced C and the N bound in the Franciscan and Western Baja Terrane metasedimentary rocks reflect the subduction or organic materials to depths approaching 40 km, with only

Table A1. Localities of Samples Analyzed in This Study[a]

Site	Latitude	Longitude
Coast Ranges-Coastal		
97-1	39.27°N	123.76°W
97-2	39.30°N	123.76°W
98-1	39.70°N	123.75°W
98-3	39.57°N	123.73°W
Coast Ranges-Central		
97-3	39.67°N	123.39°W
98-4	39.75°N	123.47°W
98-5	39.83°N	123.39°W
97-4	39.82°N	122.97°W
97-5	39.86°N	122.96°W
Coast Ranges-Eastern		
97-6	39.77°N	122.67°W
97-7	39.67°N	122.67°W
97-8	39.97°N	122.76°N
98-6	39.66°N	122.66°W
EP-4	37.07°N	121.18°W
EP-6	37.07°N	121.16°W
PP	37.05°N	121.24°W
WGE-Q20	37.06°N	121.22°W
585-1	28.19°N	115.20°W
585-14	28.12°N	115.23°W
585-14B	28.12°N	115.23°W
585-83A	28.15°N	115.23°W
585-138	28.15°N	115.13°W
486-105	28.14°N	115.38°W
585-71	28.14°N	115.18°W
585-133	28.11°N	115.21°W
585-121	28.15°N	115.15°W
585-179	28.09°N	115.22°W
486-130	28.11°N	115.35°W

[a] Latitude and longitude are presented in decimal degrees.

minor modification in concentration and isotopic composition, despite the effects of high-P/T metamorphism at temperatures of up to 250°C. Thus, although the initially organic C and N is redistributed into volatile-poor carbonaceous matter (becoming graphite at higher temperatures) and clay minerals, then higher-grade micaceous phases (as structurally bound NH_4^+), respectively, the anomalously cool subduction-zone thermal regime leads to the efficient subduction of organic C and N to at least these depths. In contrast, there is significant loss of oxidized C (calcite cement) during the low-T, high-P/T metamorphism of these rocks, as the lowest-grade rocks retain abundant calcite cement that is not present in the higher-grade rocks. It has become increasingly evident, as the result of recent field and theoretical studies of devolatilization [e.g., *Bebout*, 1995; *Kerrick and Connolly*, 2001; this study], that a large fraction of the initially subducted C reservoir (reduced and oxidized forms) is potentially preserved to great depths in subducting slabs and sediment, and that recycled C plays a significant role in the upper mantle C budget.

[41] In general, the fact that fluid-mobile trace elements (such as B, Cs, Rb, As, Sb, U, Th, S, and the LREE) are present at concentrations similar to those of their likely seafloor protoliths lends credence to approaches in which sediment geochemistry is correlated with variations in arc magma composition for these elements [see *Plank and Langmuir*, 1993, 1998]. Across-arc studies [e.g., *Ryan et al.*, 1995; *Ishikawa and Nakamura*, 1994; *Ishikawa and Tera*, 1997; *Moriguti and Nakamura*, 1998] appear to demonstrate the progressive loss profiles (and isotopic evolution) of individual elements to depths exceeding 200 km [see *Benton et al.*, 2001], thus the deeper losses are likely gradual and distributed over a significant depth range. Ultimately, knowledge of the relative efficiencies of deep subduction of seafloor components (and for some elements, isotopic evolution resulting from prograde devolatilization) obtained through study of subduction-zone metamorphic suites will aid in modeling of chemical cycling at the global scale and for individual convergent margins.

Appendix A. Localities of Samples Analyzed

[42] The localities of samples analyzed are given in Table A1.

Acknowledgments

[43] This work was funded by the National Science Foundation (EAR-9805050 to GEB) and a smaller Penrose Foundation grant 6127-97 from the Geological Society of America (to SJS). We would like to thank Gary Ernst, Angela Jayko, and J.G. Liou for assistance with field work and selection of appropriate sampling localities; and Gary Ernst and Richard Sedlock for providing additional samples for this study. We received helpful comments from Stuart Boyd (recently deceased), Tim Elliott (Associate Editor), and two Anonymous Reviewers.

References

Alt, J., and J. Burdett, Sulfur in Pacific deep-sea sediments, ODP Leg 129, and implications for cycling of sulfur in sub-

duction zone, *Proc. Ocean Drill. Program Sci. Results*, *129*, 283–294, 1992.

Alt, J. C., and D. A. H. Teagle, The uptake of carbon during alteration of ocean crust, *Geochim. Cosmochim. Acta*, *63*, 1527–1535, 1999.

Baldwin, S. L., and T. M. Harrison, Geochronology of blueschists from West-Central Baja California and the timing of uplift in subduction complexes, *J. Geol.*, *97*, 149–163, 1989.

Baldwin, S. L., and T. M. Harrison, The P-T-t history of blocks in serpentinite-matrix mélange, West-Central Baja California, *Geol. Soc. Am. Bull.*, *104*, 18–31, 1992.

Barrett, T. J., and I. Jarvis, Rare earth element geochemistry of metalliferous sediments from DSDP Leg 92: The East Pacific Rise, *Chem. Geol.*, *67*, 243–259, 1988.

Beaumont, C., S. Ellis, and A. Pfiffner, Dynamics of sediment subduction-accretion at convergent margins: Short-term modes, long-term deformation, and tectonic implications, *J. Geophys. Res.*, *104*, 17,573–17,601, 1999.

Bebout, G. E., Field-based evidence for devolatilization in subduction zones: Implications for arc magmatism, *Science*, *251*, 413–416, 1991.

Bebout, G. E., The impact of subduction-zone metamorphic processes on the mass-balance of mantle-ocean chemical exchange, *Chem. Geol.*, *126*, 191–218, 1995.

Bebout, G. E., Volatile transfer and recycling at convergent margins: mass-balance and insights from high-P/T metamorphic rocks, in *Subduction Top to Bottom*, *Geophys. Monogr. Ser.*, vol. 96, edited by G. E. Bebout et al., pp. 179–193, AGU, Washington D. C., 1996.

Bebout, G. E., and M. L. Fogel, Nitrogen-isotope compositions of metasedimentary rocks in the Catalina Schist, California: Implications for metamorphic devolatilization history, *Geochim. Cosmochim. Acta*, *56*, 2139–2149, 1992.

Bebout, G. E., and S. J. Sadofsky, $\delta^{15}N$ analyses of ammonium-rich silicate minerals by sealed-tube extractions and dual inlet, viscous-flow mass spectrometry, in *Handbook of Stable Isotope Techniques*, Elsevier, New York, in press, 2003.

Bebout, G. E., J. G. Ryan, and W. P. Leeman, B-Be systematics in subduction-related metamorphic rocks: Characterization of the subducted component, *Geochim. Cosmochim. Acta*, *57*, 2227–2237, 1993.

Bebout, G. E., E. Nakamura, and T. Nakano, Boron isotope tracers of high-temperature subduction-zone fluid processes and material recycling, *Geol. Soc. Am. Abstr. Programs*, *30*, 1841998.

Bebout, G. E., J. G. Ryan, W. P. Leeman, and A. E. Bebout, Fractionation of trace elements during subduction-zone metamorphism: Impact of convergent margin thermal evolution, *Earth Planet. Sci. Lett.*, *171*, 63–81, 1999.

Benton, L., Origin and evolution of serpentine seamount fluids, Marianna and Izu-Bonin forearcs: Implications for the recycling of subducted material, Ph.D. dissertation, Univ. Tulsa., Tulsa, Okla., 1997.

Benton, L. D., J. G. Ryan, and F. Tera, Boron systematics of slab fluids as inferred from a serpentinite seamount, Mariana forearc, *Earth Planet. Sci. Lett.*, *187*, 273–282, 2001.

Berner, R. A., A. C. Lasaga, and R. M. Garrels, The carbonate-silicate geochemical cycle and its effect on atmospheric carbon dioxide over the last 100 million years, *Am. J. Sci.*, *283*, 641–683, 1983.

Blake, M. C., A. Jayko, R. McLaughlin, and M. Underwood, Metamorphic and tectonic evolution of the Franciscan Complex, Northern California, in *Metamorphism and crustal evolution of the Western United States*, pp. 1035–1060, Prentice-Hall, Old Tappan, N. J., 1987.

Boles, J. R., and K. Ramseyer, Albitization of plagioclase and vitrinite reflectance as paleothermal indicators, San Joakin Basin, in *Studies of the Geology of the San Joakin Basin*, pp. 129–139, Soc. Econ. Paleo. Min., Los Angeles, Calif., 1988.

Bostick, N. H., Phytoclasts as indicators of thermal metamorphism, Franciscan assemblage and Great Valley Sequence (Upper Mesozoic), California, *Geol. Soc. Am. Spec. Pap.*, *153*, 1–17, 1974.

Cartigny, P., J. W. Harris, D. Phillips, M. Girard, and M. Javoy, Subduction-related diamonds?-the evidence for a mantle-derived origin from coupled $\delta^{13}C$-$\delta^{15}N$ determinations, *Chem. Geol.*, *147*, 147–159, 1998.

Cloos, M., Blueschists in the Franciscan complex of California, petrotectonic constraints on uplift mechanisms, in *Blueschists and Eclogites*, *Mem. Geol. Soc. Am.*, *164*, 77–93, 1986.

Cullers, R. L., The geochemistry of shales, siltstones and sandstones of Pennsylvanian-Permian age, Colorado, USA; Implications for provenance and metamorphic studies, *Lithos*, *51*, 181–203, 2000.

Dalla Torre, M., K. Livi, D. Veblen, and M. Frey, White K-mica evolution from phengite to muscovite in shales and shale-matrix melange, Diablo Range, California, *Contrib. Mineral. Petrol.*, *123*, 390–405, 1996.

Deines, P., The isotopic composition of reduced organic carbon, in *Handbook of Environmental Geochemistry*, pp. 239–406, Elsevier, New York, 1980.

Dumitru, T., Constraints on the uplift of the Franciscan subduction complex from apatite fission track analysis, *Tectonics*, *8*, 197–220, 1989.

Elliott, T., T. Plank, A. Zindler, W. White, and B. Bourdon, Element transport from slab to volcanic fron in the Mariana arc, *J. Geophys. Res.*, *102*, 14,991–15,019, 1997.

Ernst, W. G., Metamorphism of Franciscan tectonostratigraphic assemblage, Pacheco Pass area, east-central Diablo Range, California Coast Ranges, *Geol. Soc. Am. Bull.*, *105*, 618–636, 1993.

Evans, B., Phase relations of epidote-blueschists, *Lithos*, *25*, 3–23, 1980.

Fogel, M. L., and L. A. Cifuentes, Isotope fractionation during primary production, in *Organic Geochemistry Principles and Applications, Topics in Geobiology*, vol. 11, pp. 73–100, Plenum, New York, 1993.

Frey, M., Very low-grade metamorphism of clastic sedimentary rocks, in *Low Temperature Metamorphism*, pp. 9–58, Blackie Acad. And Prof., New York, 1987.

Frey, M., C. De Capitani, and J. G. Liou, A new petrogenetic grid for low-grade metabasites, *J. Metamorph. Geol.*, *9*, 497–509, 1991.

Fryer, P., C. Wheat, and M. Mottl, Mariana blueschist mud volcanism: Implications for conditions within the subduction zone, *Geology*, *27*, 103–106, 1999.

Grove, M., and G. E. Bebout, Cretaceous tectonic evolution of coastal southern California: insights from the Catalina Schist, *Tectonics*, *14*, 1290–1308, 1995.

Ishikawa, T., and E. Nakamura, Origin of the slab component in arc lavas from across-arc variation of B and Pb isotopes, *Nature*, *370*, 205–208, 1994.

Ishikawa, T., and F. Tera, Source, composition and distribution of the fluid in the Kurile mantle wedge: Constraints from across-arc variations and B/Nb and B isotopes, *Earth Planet. Sci. Lett.*, *152*, 123–138, 1997.

Jayko, A. S., M. C. Blake, and R. N. Brothers, Blueschist metamorphism of the eastern Franciscan belt, northern California, in *Blueschists and Eclogites*, *Mem. Geol. Soc. Am.*, *164*, 107–123, 1986.

Jayko, A., and M. C. Blake, Deformation of the eastern Franciscan Belt, Northern California, *J. Struct. Geol.*, *11*, 375–390, 1989.

Karnosov, V., N. Tseitlin, and G. Narnov, Clay minerals: Paleogeographic and diagenetic aspects, *Init. Rep. Deep Sea Drill. Proj.*, *56–57*, 979–1003, 1977.

Karpoff, A. M., Cenozoic and Mesozoic sediments from the Pigafetta Basin, Leg 129, Sites 800 and 801: Mineralogical and geochemical trends of the deposits overlying the oldest oceanic crust, *Proc. Ocean Drill. Program Sci. Results*, *129*, 3–23, 1992.

Kerrick, D. M., and K. Caldeira, Paleoatmospheric consequences of CO_2 released during early Cenozoic metamorphism in the Tethyan Orogen, *Chem. Geol.*, *108*, 201–230, 1993.

Kerrick, D. M., and J. A. D. Connolly, Metamorphic devolatilization of subducted marine sediments and transport of volatiles to the Earth's mantle, *Nature*, *411*, 293–296, 2001.

Kopf, A., and A. Dehyle, Back to the roots: Boron geochemistry of mud volcanoes and its implications for mobilization depth and global B cycling, *Chem. Geol.*, *192*, 195–210, 2002.

Kopf, A., A. Dehyle, and E. Zuleger, Evidence for deep fluid circulation and gas hydrate dissociation using boron isotopes of pore fluids in forearc sediments from Costa Rica (ODP Leg 170), *Mar. Geol.*, *167*, 1–28, 2000.

Larue, D. K., Franciscan and Cedros subduction complexes, in *Cretaceous Stratigraphy of Western North America*, edited by P. L. Abbott, pp. 211–221, Soc. Econ. Paleo. Min., Los Angeles, Calif., 1986.

Liou, J. G., S. Maruyama, and M. Cho, Very low-grade metamorphism of volcanic and volcaniclastic rocks—mineral assemblages and mineral facies, in *Low Temperature Metamorphism*, pp. 59–113, Blackie Acad., New York, 1987.

Macko, S. A., Stable isotope organic geochemistry of sediments from the Labrador Sea (sites 646 and 647) and Baffin Bay (site 645), ODP Leg 105, *Proc. Ocean Drill. Program Sci. Results*, *105*, 209–221, 1989.

Marty, B., and I. N. Tolstikhin, CO_2 fluxes from mid-ocean ridges, arcs and plumes, *Chem. Geol.*, *145*, 233–248, 1998.

McDonough, W. F., and S.-S. Sun, The composition of the Earth, *Chem. Geol.*, *120*, 223–253, 1995.

McLennan, S. M., Rare earth elements in sedimentary rocks: influence of provenance and sedimentary processes, in *Geochemistry of the Rare Earth ElementsReviews in Mineralogy*, vol. 21, pp. 169–200, Min. Soc. of Am., Boulder, Colo., 1990.

McLennan, S. M., S. R. Taylor, M. T. McCollouch, and J. B. Maynard, Geochemical and Nd-Sr isotopic-composition of deep-sea turbidites: Crustal evolution and plate tectonic associations, *Geochim. Cosmochim. Acta*, *54*, 2015–2050, 1990.

Moore, J. C., and P. Vrolijk, Fluids in accretionary prisms, *Rev. Geophys.*, *30*, 113–135, 1992.

Morad, S., Albitized microcline grains of post-depositional and probable detrital origins in Brottom Formation sandstones (Upper Proterozoic), Sparagmite Region of southern Norway, *Geol. Mag.*, *125*, 229–239, 1988.

Moran, A. E., The effect of metamorphism on the trace element composition of subducted oceanic crust and sediment, Ph.D. dissertation, Rice Univ., Houston, Tex., 1993.

Moran, A. E., V. B. Sisson, and W. P. Leeman, Boron depletion during progressive metamorphism: Implications for subduction processes, *Earth Planet. Sci. Lett.*, *111*, 331–349, 1992.

Moriguti, T., and E. Nakamura, Across-arc variations in Li isotopes in lavas and implications for crust/mantle recycling at subduction zones, *Earth Planet. Sci. Lett.*, *163*, 167–174, 1998.

Morris, J. D., W. P. Leeman, and F. Tera, The subducted component in island arc lavas: Constraints from Be isotopes and B-Be systematics, *Nature*, *344*, 31–36, 1990.

Müller, P. J., C/N ratios in Pacific deep-sea sediments: Effect of inorganic ammonium and organic nitrogen compounds sorbed by clays, *Geochim. Cosmochim. Acta*, *41*, 765–776, 1977.

Murdmaa, I., V. Gordeev, T. Kuzima, N. Turanskaya, and M. Mikhailov, Geochemistry of the Japan Trench Sediments recovered on Deep Sea Drilling Project legs 56 and 57, *Init. Rep. Deep Sea Drill. Proj.*, *56–57*, 1213–1232, 1980.

Muzuka, A. N. N., S. A. Macko, and T. F. Pedersen, Stable carbon and nitrogen isotope compositions of organic matter from sites 724 and 725, Oman Margin, *Proc. Ocean Drill. Program Sci. Results*, *117*, 571–586, 1991.

Nakano, T., and E. Nakamura, Boron isotope geochemistry of metasedimentary rocks and tourmalines in a subduction-zone metamorphic suite, *Phys. Earth Planet. Int.*, *127*, 233–252, 2001.

Noll, P. D., H. E. Newsom, W. P. Leeman, and J. Ryan, The role of hydrothermal fluids in the production of subduction zone magmas: Evidence from siderophile and chalcophile trace elements and boron, *Geochim. Cosmochim. Acta*, *60*, 587–611, 1996.

Patino, L. C., M. J. Carr, and M. D. Feingenson, Local and regional variations in Central American arc lavas controlled by variations in subducted sediment input, *Contrib. Mineral. Petrol.*, *138*, 265–283, 2000.

Peacock, S., Blueschist-facies metamorphism, shear heating, and P-T-t paths in subduction shear zones, *J. Geophys. Res.*, *97*, 17,693–17,707, 1992.

Peacock, S., Large-scale hydration of the lithosphere above subducting slabs, *Chem. Geol.*, *108*, 49–59, 1993.

Peacock, S., Thermal and petrologic structure of subduction zones, in *Subduction Top to Bottom*, *Geophys. Monogr. Ser.*,

vol. 96, edited by G. E. Bebout, pp. 119–133, AGU, Washington D. C., 1996.

Pickering, K. T., N. G. Marsh, and B. Dickie, Data Report: Inorganic major, trace, and rare earth element analyses of the muds and mudstones from site 808, *Init. Rep. Deep Sea Drill. Proj.*, *131*, 427–450, 1993.

Plank, T., and C. H. Langmuir, Tracing trace elements from sediment input to volcanic output at subduction zones, *Nature*, *362*, 739–743, 1993.

Plank, T., and C. H. Langmuir, The chemical composition of subducting sediment and its consequences for the crust and mantle, *Chem. Geol.*, *145*, 325–394, 1998.

Rau, G. H., M. A. Arthur, and W. E. Dean, $^{15}N/^{14}N$ variations in Cretaceous Atlantic sedimentary sequences: Implications for past changes in marine nitrogen biogeochemistry, *Earth Planet. Sci. Lett.*, *82*, 269–279, 1987.

Rea, D. K., and L. J. Ruff, Composition and mass flux of sedimentary materials entering the world's subduction zones: Implications for global sediment budgets, great earthquakes, and volcanism, *Earth Planet. Sci. Lett.*, *140*, 1–12, 1996.

Richet, P., Y. Bottinga, and M. Javoy, A review of hydrogen, carbon, nitrogen, oxygen, sulphur, and chlorine stable isotope fractionation among gaseous molecules, *Annu. Rev. Earth Planet. Sci.*, *5*, 65–110, 1977.

Ryan, J., and C. H. Langmuir, The systematics of boron abundances in young volcanic rocks, *Geochim. Cosmochim. Acta*, *57*, 1727–1741, 1993.

Ryan, J., J. Morris, F. Tera, W. P. Leeman, and A. Tsvetkov, Cross-arc variations in geochemical parameters in the Kurile Arc as a function of slab depth, *Science*, *270*, 625–627, 1995.

Ryan, J., J. Morris, G. Bebout, and W. P. Leeman, Describing chemical fluxes in subduction zones: insights from "depth profiling" studies of arc and forearc rocks, in *Subduction Top to Bottom*, *Geophys. Monogr. Ser.*, vol. 96, edited by G. E. Bebout, pp. 263–268, AGU, Washington D.C., 1996.

Sadofsky, S. J., and G. E. Bebout, Ammonium partitioning and nitrogen-isotope fractionation among coexisting micas during high-temperature fluid-rock interactions: Examples from the New England Appalachians, *Geochim. Cosmochim. Acta*, *64*, 2835–2849, 2000.

Sadofsky, S. J., and G. E. Bebout, Paleohydrogeology at 5 to 50 kilometer depths of accretionary prisms: The Franciscan Complex, California, *Geophys. Res. Lett.*, *28*, 2309–2312, 2001a.

Sadofsky, S. J., and G. E. Bebout, Nitrogen geochemistry of subducting sediments: New results from the Western Pacific, *Eos Trans. AGU*, 2001b.

Sano, Y., and S. N. Williams, Fluxes of mantle subducted carbon along convergent margins, *Geophys. Res. Lett.*, *23*, 2749–2752, 1996.

Sedlock, R. L., Metamorphic petrology of a high pressure, low temperature subduction complex in West-Central Baja California, Mexico, *J. Metamorph. Geol.*, *6*, 205–233, 1988.

Sedlock, R. L., Syn-subduction forearc extension and blueschist exhumation in Baja California, Mexico, in *Subduction Top to Bottom*, *Geophys. Monogr. Ser.*, vol. 96, edited by G. E. Bebout, pp. 155–162, AGU, Washington D.C., 1996.

Seewald, J. S., W. E. Seyfried, and E. C. Thornton, Organic-rich sediment alteration: an experimental and theoretical study at elevated temperatures and pressures, *Appl. Geochem.*, *5*, 193–209, 1990.

Spivack, A. J., M. R. Palmer, and J. M. Edmond, The sedimentary cycle of the boron isotopes, *Geochim. Cosmochim. Acta*, *51*, 1939–1949, 1987.

Staudigel, H., S. R. Hart, H. U. Schmincke, and B. M. Smith, Cretaceous ocean crust at DSDP Sites 417 and 418: carbon uptake from weathering versus loss by magmatic outgassing, *Geochim. Cosmochim. Acta*, *53*, 3091–3099, 1989.

Sturtz, A., Experiments on hydrothermal reactions between hemipelagic sediments and seawater, Ph.D. dissertation, Univ. of Calif., San Diego, 1991.

Sweeney, R. E., K. K. Liu, and I. R. Kaplan, Oceanic nitrogen isotopes and their uses in determining the source of sedimentary nitrogen, in *Stable Isotopes in the Earth Sciences*, DSIR Bull. 220, pp. 9–26, Sci. Info. Div., New Zealand, 1978.

Tagami, T., and T. Dumitru, Provenance and thermal history of the Franciscan accretionary complex, *J. Geophys. Res.*, *101*, 11,353–11,364, 1996.

Taylor, S. R., and S. M. McLennan, The continental crust: Its composition and evolution, Blackwell, Malden, Mass., 1985.

Teichmüller, M., Organic material and very low-grade metamorphism, in *Low Temperature Metamorphism*, pp. 114–161, Blackie Acad. and Prof., New York, 1987.

Terabayashi, M., and S. Maruyama, Large pressure gap between the Coastal and Central Franciscan Belts, northern and central California, *Tectonophysics*, *285*, 87–101, 1998.

Terabayashi, M., S. Maruyama, and J. G. Liou, Thermobaric structure of the Franciscan Complex in the Pacheco Pass region, Diablo Range, California, *J. Geol.*, *104*, 617–636, 1996.

Underwood, M. B., and S. B. Bachman, Sandstone petrofacies of the Yager Complex and the Franciscan Coastal Belt, Paleogene of northern California, *Geol. Soc. Am. Bull.*, *97*, 809–817, 1986.

Underwood, M. B., and X. Deng, Clay mineralogy and clay geochemistry in the vicinity of the décollement zone, northern Barbados Ridge, *Proc. Ocean Drill Program Sci. Results*, *156*, 3–30, 1997.

von Huene, R., and D. W. Scholl, Observations at convergent margins concerning sediment subduction, subduction erosion, and the growth of continental crust, *Rev. Geophys.*, *29*, 279–316, 1991.

Vrolijk, P. J., S. R. Chambers, J. M. Gieskes, and J. R. O'Neil, Stable isotope ratios of interstitial fluids from the Northern Barbados accretionary prism, ODP Leg 110, *Proc. Ocean Drill. Program Sci. Results*, *110*, 189–205, 1990.

Waples, D. W., and R. Cunningham, Leg 80 shipboard organic geochemistry, *Init. Rep. Deep Sea Drill. Proj.*, *80*, 949–968, 1985.

Waples, D. W., and J. R. Sloan, Carbon and nitrogen diagenesis in deep-sea sediments, *Geochim. Cosmochim. Acta*, *44*, 1463–1470, 1980.

You, C.-F., P. R. Castillo, J. M. Gieskes, L. H. Chan, and A. J. Spivack, Trace element behavior in hydrothermal experiments: Implications for fluid processes at shallow depths in subduction zones, *Earth Planet. Sci. Lett.*, *140*, 41–52, 1996.